



8-2009

Investigation of the Chemical and Physical Properties of Asian Dust and Asian Pollution Transpacific Transport During the Intex-B Field Campaign

Timothy S. Logan

Follow this and additional works at: <https://commons.und.edu/theses>



Part of the [Psychology Commons](#)

Recommended Citation

Logan, Timothy S., "Investigation of the Chemical and Physical Properties of Asian Dust and Asian Pollution Transpacific Transport During the Intex-B Field Campaign" (2009). *Theses and Dissertations*. 884.

<https://commons.und.edu/theses/884>

This Thesis is brought to you for free and open access by the Theses, Dissertations, and Senior Projects at UND Scholarly Commons. It has been accepted for inclusion in Theses and Dissertations by an authorized administrator of UND Scholarly Commons. For more information, please contact zeineb.yousif@library.und.edu.

INVESTIGATION OF THE CHEMICAL AND PHYSICAL PROPERTIES OF ASIAN
DUST AND ASIAN POLLUTION TRANSPACIFIC TRANSPORT DURING THE
INTEX-B FIELD CAMPAIGN

by

Timothy S. Logan
Bachelor of Arts, University of Virginia, 1993

A Thesis
Submitted to the Graduate Faculty

of the

University of North Dakota

in partial fulfillment of the requirements

for the degree of

Master of Science

Grand Forks, North Dakota

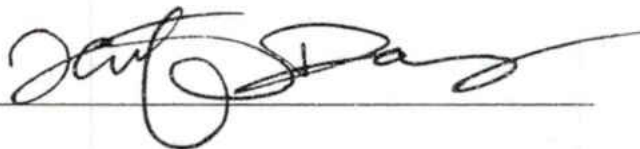
August
2009

Copyright 2009 Timothy S. Logan

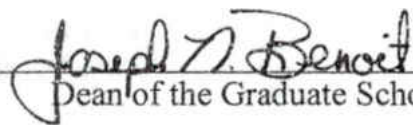
This thesis, submitted by Timothy S. Logan in partial fulfillment of the requirements for the Degree of Master of Science from the University of North Dakota, has been read by the Faculty Advisory Committee under whom the work has been done and is hereby approved.



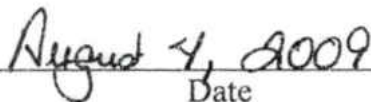
Chairperson



This thesis meets the standards for appearance, conforms to the style and format requirements of the Graduate School of the University of North Dakota, and is hereby approved.



Dean of the Graduate School



Date

PERMISSION

Title Investigation of the Chemical and Physical Properties of Asian Dust and Asian Pollution Transpacific Transport during the INTEX-B Field Campaign

Department Atmospheric Sciences

Degree Master of Science

In presenting this thesis in partial fulfillment of the requirements for a graduate degree from the University of North Dakota, I agree that the library of this University shall make it freely available for inspection. I further agree that permission for extensive copying for scholarly purposes may be granted by the professor who supervised my thesis work or, in his absence, by the chairperson of the department or the dean of the Graduate School. It is understood that any copying or publication or other use of this thesis or part thereof for financial gain shall not be allowed without my written permission. It is also understood that due recognition shall be given to me and to the University of North Dakota in any scholarly use which may be made of any material in my thesis.

Signature



Date

7/22/2009

TABLE OF CONTENTS

LIST OF FIGURES	vii
LIST OF TABLES	ix
ACKNOWLEDGEMENTS	x
ABSTRACT	xi
CHAPTER	
I. INTRODUCTION	1
II. DATA AND METHODOLOGY	17
Instrumentation	17
DIAL	18
Nephelometer	19
Ion and Gas Chromatography	21
Diode Laser Spectrometry	22
Chemiluminescence	23
Methodology	24
Define the area for this study	24
Define the dust and pollution plume	25
The First Scientific Question	26
The Second Scientific Question.....	28
III. RESULTS	34
The First Scientific Question	34

Case I	43
Case II	43
Cases III and IV	44
Discussion	45
The Second Scientific Question.....	53
Clean Case.....	53
Results and Discussion.....	56
The Third Scientific Question.....	59
Comparison of the dust and pollution vertical distributions among the 3 field experiments at remote Pacific region..	59
Relationship between PAN and Ozone within the dust plume.....	63
IV. CONCLUSIONS	64
REFERENCES	69

LIST OF FIGURES

Figure	Page
1. Source region of Asian dust, the Gobi desert located between north-central China and Mongolia, and Tibet plateau located western China.	2
2. The April 1998 "Perfect Dust Storm" which affected eastern Asia, the Pacific Ocean and the United States (Image from Husar et al. 1998).....	3
3. Heterogeneous pathways for Sulfur Dioxide conversion to Sulfate	8
4. Summary of the sampling regions of the PEM-B (1994) Campaign.....	14
5. Summary of the sampling regions of the PEM-B (1994) and TRACE-P (2001) Campaigns.....	14
6. Summary of INTEX-B Flight Tracks with Region Bin Overlay	24
7. Mechanism for reaction of Asian dust with gas and solid phase pollution within the plume.....	30
8. Description of fine mode and soluble sulfate during Step C	30
9. DIAL Plots for April 17, April 23, and April 25	35
10. DIAL Plots for April 28, May 1 and May 4.....	36
11. DIAL Plots for May 7 and May 9	37
12. DIAL Backscattering Ratio Plots for the Four "In Plume" Case Studies and the Clean Case.....	38
13. Depolarization Plots during the case study time dates and time intervals	39

14.	(a) The scattering coefficients at three wavelengths (450, 550, and 700 nm), (b) calcium ion concentration, (c) fine sulfate concentration, and (d) the Angström exponent α observed by the TSI Model 3563 nephelometer onboard the DC-8 aircraft on April 17, 2006. For the April 24 case, (e-h) are the same as (a-d).	41
15.	Two April 29 cases. (a) The scattering coefficients at three wavelengths (450, 550, and 700 nm), (b) calcium ion concentration, (c) fine sulfate concentration, and (d) the Angstrom exponent α observed by the TSI Model 3563 nephelometer onboard the DC-8 aircraft on April 17, 2006. (e-h) are the same as (a-d).....	42
16.	HYSPLIT Backward Trajectory Plot for Case I	47
17.	HYSPLIT Backward Trajectory Plot for Case II.....	48
18.	HYSPLIT Backward Trajectory Plot for Case III	49
19.	HYSPLIT Backward Trajectory Plot for Case IV	50
20.	Depiction of a Flight Track Passing Through a Poorly Mixed Plume (a) and Well Mixed Plume (b) and the Corresponding Fine Aerosol Data over Time	53
21.	April 17 Case	54
22.	April 24 Case	55
23.	April 29 First Plume Case	55
24.	April 29 Second Plume Case	56
25.	Vertical distribution of mean Asian dust and pollution values over the remote eastern Pacific.	61
26.	Temporal Relationship between PAN and Ozone in April 29 Case	62
27.	Statistical Correlation of P_t N with Ozone during the April 29 Case	63

LIST OF TABLES

Table	Page
1. Annual Means and Standard Deviations of α Measured at Sites in the Chinese Sun Hazemeter Network (CSHNET).....	28
2. Summary of Chemical and Physical Properties of the Four Cases and Their Uncertainties as Given by Standard Deviations (σ).....	51
3. Mean Unreacted Dust Fractions for Cases I-IV	57

ACKNOWLEDGEMENTS

Thank you to my beloved grandmother and my family for shaping my mind through the years. Thank you to all my friends at Morris School District in New Jersey who believed in me and helped me to realize that learning should always be lifelong, meaningful, and challenging. Thank you to my advising committee of Dr. Baike Xi, Dr. Jianglong Zhang, and Dr. Xiquan Dong, and a special thanks to Dr. David Delene for their guidance, expertise, and support. Thank you to all the graduate students in the Atmospheric Sciences Department especially those in my research group, Rebecca Obrecht, Aaron Kennedy, Kathryn Crosby, Zhe Feng, Hongchun Jin, Yingxi Shi, Di Wu, and fellow Class of 2009 graduate students Dan Adriaansen, Adam Theissen, Amanda Homann, and Jennifer Green for all the good times and helping me with numerous computer programming issues.

This work was partially supported by the North Dakota Space Grant Consortium. The UNH/NASA ion data (Dr. Jack Dibb, PI), sulfur dioxide (Dr. Greg Huey, PI), carbon monoxide (Dr. Glen Sachse, PI), ozone (Dr. Melody Avery, PI), PAN (Dr. Hanwat Singh, PI), DC-8 DIAL (Dr. Edward V. Browell, PI), and nephelometer (Dr. Antony Clarke, PI, and Dr. Yohei Shinozuka) data were downloaded from the NASA LaRC INTEX-B website (<http://www-air.larc.nasa.gov/cgi-bin/arcstat-b>). The HYSPLIT transport model was provided by the NOAA Air Resources Laboratory (ARL) and can be found at the READY website (<http://www.arl.noaa.gov/ready.html>).

ABSTRACT

Asian dust events during INTEX-B were analyzed by using chemical and physical *in situ* measurements taken by instruments on board a NASA DC-8 aircraft during the INTEX-B (2006) field campaign. From this analysis, the three following scientific questions about the nature of the Asian dust events were answered: (1) How can we identify which mode dominates in the observed dust plumes, (2) How do the pollutants and Asian dust interact with each other to form secondary pollutants, and (3) Has the pollution measured over the remote Pacific increased over the time interval of two previous field experiments (PEM-B 1994 and TRACE-P 2001) that conducted research of Asian dust and pollution over the western remote Pacific.

For the first question, DIAL measurements at 588 and 1064 nm can roughly define the dust/pollution plume boundary. The magnitude of wavelength dependence of the aerosol scattering ratios at 450, 550 and 700 nm as measured by the nephelometer demonstrates whether the plume contains fine mode aerosols; which is believed to be an excellent indicator of whether the Asian dust plume is carrying any pollution along its transport pathway. Based on the wavelength dependence, three types of Asian dust plumes were identified: (a) Type I - a plume dominated by coarse mode aerosol, which is weakly dependent on wavelength (dust), (b) Type II - a plume dominated by fine mode aerosol, which is strongly dependent on wavelength (pollution), and (c) Type III - two plumes that contained a mixture of both Asian dust and pollution.

A HYSPLIT backward trajectory model was used to verify the origins of these dust plumes as crossing through desert regions, regions of large urban populations, as well as mixtures of both. Chemical data derived from ion and gas chromatography was used to show the tracers of dust (calcium ions), aqueous phase pollution (sulfate and nitrate ions) and gas phase pollution (sulfur dioxide).

The second question focused on gas to particulate phase reactions (fine mode to coarse mode pollution conversions) and used the same four plume cases as the first question. Types I and II had 16 and 18 pptv sulfur dioxide, respectively, while Type III had 78 and 93 pptv, respectively. Both the strong dust and strong pollution cases showed a more complete conversion where the two mixture cases suggested incomplete gas to particulate phase reactions at the point where the aircraft intercepted the plume. To answer the third question, a technique adopted by Dibb et al. (1996, 1997, and 2003) was used to show whether pollution has increased over the three field campaigns. Though the data shows an inherent increase, there is no conclusive evidence for a possible pollution increase since no observations from the source regions exist for the purpose of this study. Therefore, the observed increased trends may be due to better sampling techniques and methods developed for the INTEX-B 2006 field campaign.

CHAPTER I

INTRODUCTION

Both the rapid urbanization and industrialization taking place in Asia are expected to have considerable effects on the physical and chemical properties of the atmosphere. However, these implications are not confined locally or regionally since transport and chemical evolution of trace gases and aerosols from the Asian continent significantly alter the atmospheric composition over the remote Pacific (Dibb et al. 2003, Zhang et al. 2003). There is growing evidence of Asian pollution and aerosol transport capable of reaching North America (Jaffe et al. 1999). Asia is one of the most significant sources of aerosol particles on our planet (Stith et al. 2009). However, quantitative studies of the global transport of Asian pollution are ad hoc issues in order to address their global impact on air quality, human health, and our climate.

Asian dust storms are extreme aerosol loading events that tend to produce large quantities of dust, smoke, or haze, which are then dispersed over regional or global scales. These easily observable particles can illustrate and quantify the nature of transport, transformation, and removal processes along their path (Husar et al. 1998). Though the dust storms occur at different time periods during the course of the year, they are usually stronger in the spring months. During the spring, the north central and eastern regions of Asia are plagued by strong, sporadic dust events. These events are natural phenomena that originate in the Gobi desert region between north-central China and Mongolia as shown in Figure 1.



Figure 1: Source region of Asian dust, the Gobi desert located between north-central China and Mongolia, and Tibet plateau located western China.

The dust events are caused by strong surface winds and large-scale low-pressure synoptic patterns that are capable of disturbing and lifting large amounts of fine, dry soil/sand particles into the free atmosphere. The transport process is also capable of lofting anthropogenic pollution along with the dust plumes. Rapid increases in industrialization in Asia have led to an increase in the amount of pollution being lofted into the dust plumes. Remarkably, the increase in both urbanization and industrialization on the Asian continent in the past decades has added an abundance of anthropogenic aerosols to the atmosphere (Xin et al. 2007). As these plumes are carried eastward by prevailing winds, they pass over the polluted regions and draw up large concentrations of aerosols and other pollutants into the free troposphere. Therefore, the Asian dust events

provide a unique opportunity to examine the intercontinental transport and evolution of Asian pollution.

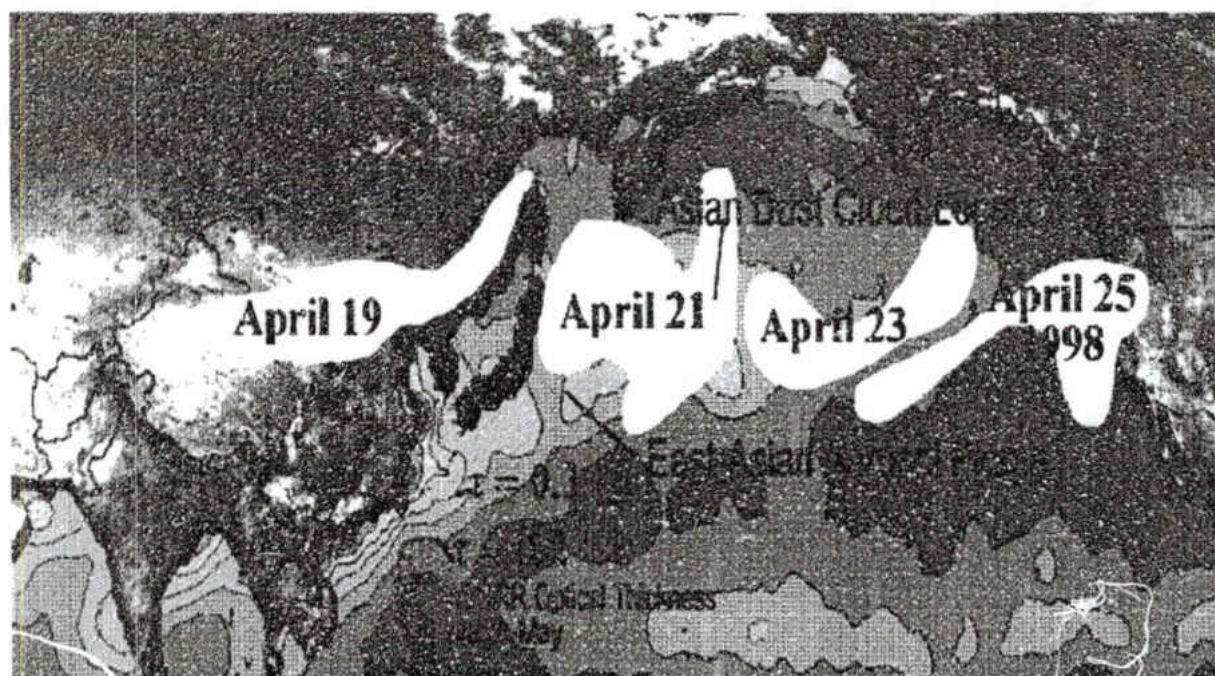


Figure 2: The April 1998 "Perfect Dust Storm" which affected eastern Asia, the Pacific Ocean and the United States (Image from Husar et al. 1998)

Over the duration of the plume transport, the mixture of Asian dust and pollution affect air quality in the areas of north-eastern Asia (North and South Korea, eastern China, Japan, and extreme eastern Russia). At times, the pollutant laden plumes can transport aerosols across the Pacific Ocean, and eventually impact the areas of North America such as the United States and Canada (Husar et al. 1998, Jaffe et al. 1999). A transport event that occurred in April 2001, deemed the largest Asian dust event ever observed at the time, was observed and studied by Jaffe et al. (1999). They investigated the influence of this event on the atmospheric boundary layer over the United States and concluded that extreme episodes of intercontinental transport can adversely affect air quality in regions further downwind from the original emission source (Jaffe et al. 2003).

The decline in air quality as a result anthropogenic pollution is one of the biggest environmental problems human beings face on Earth. Strict environmental laws have been enacted to remediate air quality in most industrialized nations (e.g. the United States, Canada, Japan, and Europe) such that factory effluents are treated before they are discharged into the atmosphere. However, there are cases where the laws of neighboring upwind countries are either less strict or have yet to be enacted.

The pollution within the dust plume can undergo various reactions and generate secondary chemical species that can be far worse than their precursors. Jacob et al. (1999) conducted a study on the effect of rising Asian emissions on current ozone levels in the United States. As a result of the ongoing increase in Asian pollution, they expected an increase of ozone concentrations in a range of 2-6 ppbv in the western United States by 2010 (Jacob et al. 1999). The western United States is continuously plagued by poor air quality due to frequent episodes of inversion layers that cause air stagnation and trap automobile exhaust and factory effluent near the Earth's surface. These inversions occur as a result of a combination of varying wind patterns and the topography of the west coast.

Human health is also affected by the mixed Asian dust and pollution transport. The smog and haze that blanket large urban areas cause severe health ailments among susceptible populations. It is generally accepted that severe air pollution episodes, characterized by high levels of aerosols and sulfur dioxide, are associated with substantial excess mortality (Ware et al. 1981). Chen et al. (2003) conducted a study relating Asian dust storm events to daily mortality rates in Taiwan, and concluded a causal relationship between increased particulate matter and combustion related pollutants (sulfur dioxide,

nitrogen dioxide, and carbon monoxide) with excess daily mortality during the dust events. Circulatory related deaths rose 2.59% while respiratory deaths rose 7.66% within 48 hours after the dust events had passed (Chen et al. 2003).

A number of studies had pointed out that the overall increase in percentages of mortalities due to dust events was not statistically significant, but the increases in mortality rates during the dust storms could not be explained otherwise. They also took into account the number of conflicting studies as to which mode of pollution (e.g., fine vs. coarse mode) causes the most distress (Schwartz et al. 1996; Levy et al. 2000; Dockery et al. 1992; Castillejos et al. 2000). A similar study conducted by Yoo et al. (2008) relating Asian dust events to asthmatic children in South Korea, yielded similar results. They found increased respiratory distress during the dust events with extreme cases of distress requiring hospitalization within 48 hours of the events' passing. In both of these cases, the polluted air originated from upwind sources in northern and central Asia.

Asian dust plumes can reduce the incoming solar radiation reaching the ground (i.e. the so called the aerosol direct effect). An example of the direct effect is the "Perfect Dust Storm" in April 1998 where the dust plume significantly enhanced the optical depth of the atmosphere, increased the solar radiation reflected back to space, and appreciably decreased incoming solar radiation at the surface which lead to an alteration of the heating profile in the atmosphere. This strong dust event created an enormous dust plume that exited the Asian mainland and traveled across the Pacific to the United States (Fig. 2). Another piece of evidence was the 30% reduction of direct solar radiation, observed at the AERONET stations in the western United States (Obrecht 2008).

The aerosol indirect effect is due to the portion of soluble aerosols that serves as cloud condensation nuclei, alter the cloud formation/dissipation processes, and increase the lifetime of clouds (Albrecht 1989). The increasing number concentration of cloud droplets along with a reduction in their size can lead to an increase in optical depth and a decrease in the amount of incoming solar radiation to the ground. Leaitch et al. (2009) examined the effects of intermixed Asian dust and pollution on the formation of cloud condensation nuclei and concluded the coarse particles of dust act to accumulate sulfate, nitrate, and other particles which diminishes the roles of these species in indirect radiative forcing but potentially enhances their roles in direct radiative forcing.

The primary Asian pollution can be categorized by its source, (industrial emission, biomass burning), or its phase (gas phase, such as SO_2 , NO_x , CO, O_3 , etc; particulate phase, sulfate, nitrate, soot, etc). These compounds may involve further reactions to form new species, especially, the gas phase species may be taken up by the aqueous particles to form the secondary aerosols. Secondary aerosols generated from the interactions of Asian pollution and dust along the transport pathways even further alters the chemical nature of the troposphere (Leaitch et al. 2009).

The formation of secondary aerosols is dominated by heterogeneous processes that take place on the surfaces of Asian dust particles. Studies have shown that insoluble calcium salts, such as calcium oxide and calcium carbonate (CaO and CaCO_3) present in Asian dust can facilitate the oxidation of SO_2 and NO_x species to coarse mode sulfate and nitrate. During transport across the remote Pacific, the calcium carbonate fraction in the dust can be converted to calcium sulfate or calcium nitrate as the gas phase precursors condense as acid aerosols on the dust particles (McNaughton et al. 2009). Calcium

silicate and aluminosilicate minerals are also present in Asian dust at relative amounts of 12 and 68%, respectively. However, these calcium species are far less reactive and will generate fewer calcium ions in the presence of acid aerosols. Naturally occurring chemical radicals, such as hydroxyl (OH^\cdot) and peroxyhydroxyl (HO_2^\cdot) radicals, also help facilitate these reactions by supplying the extra oxygen atoms needed for oxidation. The detailed pathways that illustrate the heterogeneous reactions of gas phase pollutants are discussed as follows.

Sulfur dioxide is a primary constituent of man-made pollution and is responsible for the majority of sulfate based aerosols observed in the Asian dust plumes. The mechanism for sulfate production is heterogeneous in nature but can go in two different directions: gaseous to aqueous pathway or a pathway including gaseous, aqueous and solid phases terminating in the solid phase as illustrated in Figure 3.

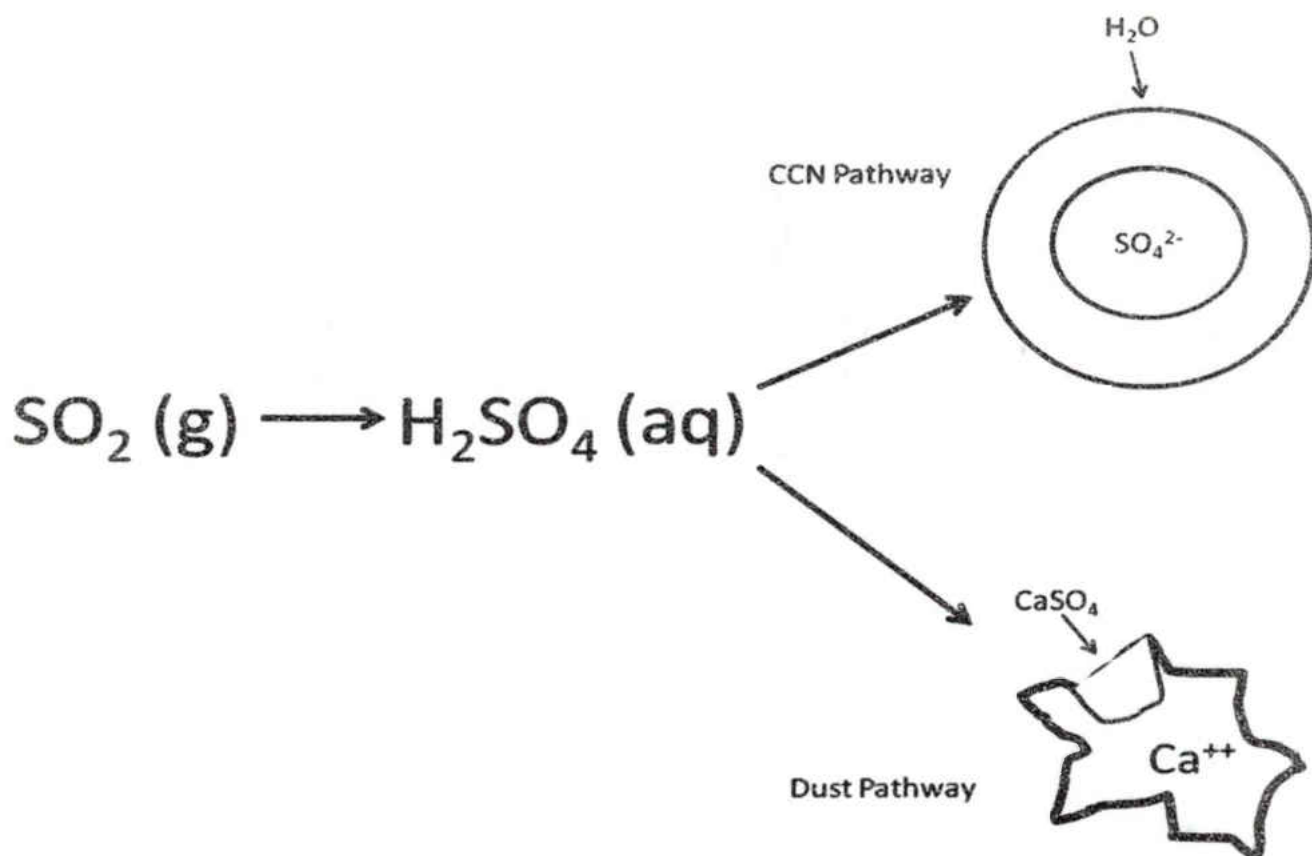


Figure 3: Heterogeneous pathways for Sulfur Dioxide conversion to Sulfate.

Calcite (CaCO_3), the chief source of reactive (free) calcium ions in Asian dust, is reported to make up anywhere from 3.6 – 21% of the mineral composition of Asian dust (Liu 1985).

The reaction mechanism is described as follows:



and



If M represents water droplets or other aqueous phase species, then the resulting sulfate aerosol will remain suspended and can become nuclei for cloud condensation. If M represents solid phase species such as dust particles (Asian dust in particular), then the resulting sulfate will react with the chemical species present in the dust (primarily calcium) and form a soluble sulfate coating. The removal of sulfates from the atmosphere is either by precipitation scavenging when the sulfates act as CCN or by gravitational settling when the sulfates become bound to the mineral dust lattices. The former will tend to form fine mode aerosols and the latter will form coarse mode ones.

Nitrogen oxides are a class of gaseous nitrogenous species that are extremely reactive. They include nitric oxide (NO), dinitrogen dioxide (N₂O₂), nitrous oxide (N₂O), nitrogen dioxide (NO₂) and dinitrogen pentoxide (N₂O₅). Some are photochemically reactive when they are exposed to ultraviolet radiation, and release single oxygen atoms that act as radicals and form other secondary compounds (e.g. production of stratospheric ozone via the Chapman cycle). They can all oxidize to form nitric acid and subsequently nitrate aerosol through a pathway very similar to sulfur dioxide.



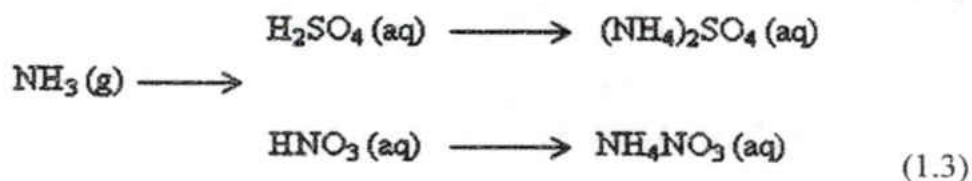
and



Again if M is an aqueous species, submicron nitrate aerosols will form as opposed to supermicron aerosols that are formed as a result of nitric acid reacting with the calcium compounds in the dust. Fine nitrate normally does not serve as CCN in contrast to fine

sulfate. Once aqueous phase nitrate aerosols form, they will either react with ammonium to form ammonium nitrate (NH_4NO_3) aerosols or be scavenged by wet removal processes such as precipitation events (Jordan et al. 2003). Coarse mode nitrate is removed by the same process as coarse mode sulfate, which is by dry deposition.

Ammonia gas is the third most abundant nitrogen containing gas in the atmosphere. It is usually the waste product of biological processes that occur within nearly all living organisms and is found in abundance in the atmosphere, land, and ocean. Though it is only one of the chemical tracers as being biogenic source, the amount of ammonia released by anthropogenic activities, such as agriculture and industry, rivals that of natural sources. Ammonia is also the only constituent in the atmosphere that can neutralize the acidic gaseous oxides of sulfur and nitrogen, thus removing them from the atmosphere. When observed within Asian dust plumes, the ammonium species are usually indicators of reactions between ammonia and the gaseous precursors on dust surfaces (Jordan et al. 2003). Many power plants and factories utilize ammonia gas to treat and neutralize acid gas effluent (e.g. SCR process). This offers an explanation as to why ammonium ions are usually presented with sulfates and nitrates in pollution plumes (Dibb et al. 2003). These reactions are heterogeneous because gaseous ammonia can readily form ammonium ions in the presence of moisture, and then the ammonium ions react with sulfur dioxide and nitrogen dioxide to form ammonium sulfate and nitrate species as follows:



Carbon monoxide (CO) is a byproduct of the combustion of volatile organic carbon (VOC) compounds found in fossil fuels and biomass burning. It can also be formed by the photo-oxidation of anthropogenic methane in the free atmosphere. The major source of carbon monoxide in the atmosphere is not well understood though anthropogenic processes are dominant as it is estimated that approximately two-thirds of total CO comes from anthropogenic activities. CO has a long residence time as compared to other gaseous tracers and is slow in reacting to form secondary aerosols (its primary removal process is reactions with OH radicals). Therefore, it is a good tracer of pollution because it remains relatively invariant in concentration during the transport process of Asian pollution within the Asian dust plumes.

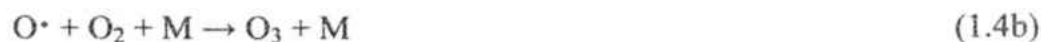
Ozone exists in several layers of the atmosphere. Stratospheric ozone production via the Chapman mechanism is given as



and

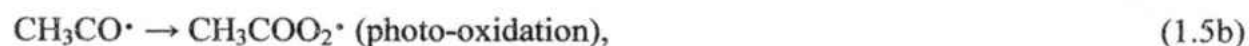


where the oxygen radical (O^\bullet) is extremely reactive with other diatomic oxygen molecules to form ozone. A suggested tropospheric ozone mechanism involves the photochemical reaction between reactive nitrogen species given by



Ozone created in the middle to lower troposphere is usually branded a pollutant. During the daytime, ozone termed as “in situ” is generated by the photodecomposition of reactive nitrogenous compounds that release oxygen radicals into the atmosphere. These reactive compounds are most often associated with anthropogenic pollution and are responsible for the photochemical smog incidents that constantly plague many urban areas on Earth.

One class of reactive nitrogenous compounds being scrutinized in recent studies is peroxyacetyl nitrate (PAN) (Jacob et al. 1999). PAN ($\text{CH}_3\text{COO}_2\text{NO}_2$) is formed by the reaction of two-carbon volatile organic hydrocarbons (VOC) with oxygen and nitrogen dioxide as follow:



and



It is formed usually in the daytime through homogeneous photochemical mechanisms but can decompose into VOCs, NO_2 , and oxygen radicals during the night. Since NO_2 and radical oxygen are important species in ozone generation, PAN serves as

a facilitator for ozone production in the troposphere and thus indirectly contributes to high concentrations of ozone.

Previous studies related to the transpacific transport of Asian dust and pollution, such as the 1994 **Pacific Exploratory Mission West Phase B** (PEM-B 1994) and the 2001 **Transport and Chemical Evolution over the Pacific** (TRACE-P 2001), have found links between dust events and a possible increase in both strength and distance of pollution transport. Although Asian pollution and dust can occur year around, the dust events are more prevalent during spring months than other seasons (Dibb et al. 1997). This was the main finding of the PEM-B (1994) study as analyzed by Dibb et al. (1997). The TRACE-P (2001) campaign did more extensive sampling of Asian dust outflow and concluded that the observed increase in Asian pollution could not be explained by stronger storms or lack of scavenging (Dibb et al. 2003). However, these studies were conducted in close proximity to the Asia and in the vicinity of the western Pacific Ocean as shown in Figures 4 and 5.

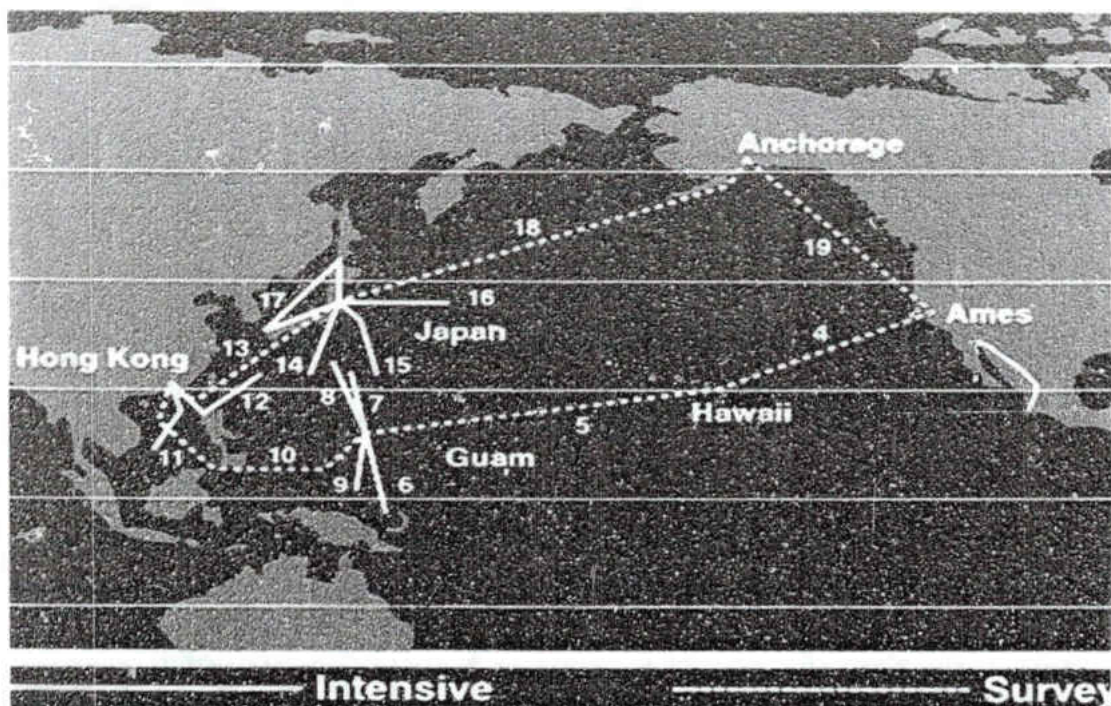


Figure 4: Summary of the sampling regions of the PEM-B (1994) Campaign



Figure 5: Summary of the sampling regions of the PEM-B (1994) and TRACE-P (2001) Campaigns

In 2006, a NASA led field campaign, INTEX-B (**I**ntercontinental Chemical Transport Experiment – Phase **B**), was conducted during a 12-week period from March 1st to May 15th over Mexico and over the remote Pacific Ocean. This campaign was

divided into two parts: (a) study pollution outflow from Mexico City to the United States (Part I) and (b) study Asian dust and pollution inflow to the United States via the Pacific Ocean (Part II). The INTEX-B study contained a wealth of chemical and physical data taken from instruments on board a NASA DC-8 aircraft. Both parts aimed to understand the transport and transformation of gases and aerosols on transcontinental and intercontinental scales as well as assess their impact on air quality and climate (Singh et al. 2005). The second part of the INTEX-B (2006) field campaign was chosen as a basis for this study because it involved sampling more over the eastern Pacific and closer to the United States.

Part II of INTEX-B targeted the following five main goals: (1) to quantify the transpacific transport and evolution of Asian pollution to North America and assess its implications for regional air quality and climate, (2) to investigate the transport of Asian to North America and assess its implications for American air quality, (3) to validate and refine satellite observations of tropospheric composition, and (4) to map emissions of trace gases and aerosols and relate atmospheric composition to sources and sinks (Singh et al. 2005). This study will focus mainly on data taken from DC-8 in-situ measurements over the remote regions of eastern Pacific Ocean.

Physical and chemical approaches are used in this study to address the following three scientific questions:

(1) How can we identify which mode (fine or coarse) dominates in the observed dust plumes?

(2) How do the pollutants and Asian dust interact each other to form secondary pollutants (i.e. explain and quantify various heterogeneous chemical reactions within the

dust plume)? Does the presence of Asian dust catalyze the conversion of gas phase pollutants to particle phase ones?

(3) Whether the pollution measured over the remote Pacific has increased since the early 1990s during PEM-WEST B (1994) and TRACE-P (2001) field experiments?

To answer the above three questions, we have set up three objectives, respectively, in this study as: (1) investigating the microphysical properties of the Asian dust as related to Asian pollution, (2) examining the chemical constituents and interactions pollutants derived from Asian pollution present within the dust plumes, and (3) investigating the dust and pollution differences within the remote Pacific among these three field experiments.

CHAPTER II

DATA AND METHODOLOGY

Instrumentation

The data used for this study was taken solely from DC-8 aircraft measurements over the eastern Pacific Ocean. A brief description of the instruments includes: (a) for physical properties of the plume – Differential Absorption Lidar (DIAL) and nephelometer, and (b) for chemical properties of the plume – ion chromatography, gas chromatography, mass spectrometry, diode laser spectroscopy, and chemiluminescence data. The types of measurements used in this study include: (1) pressure altitude, longitude, and latitude (i.e., flight track), (2) physical properties – aerosol scattering ratios at 550 and 1064 nm from DIAL, aerosol scattering coefficients at 450, 550, and 700 nm from nephelometer, and Angström exponent and spectral curvature values inferred from nephelometer, and (3) chemical properties – bulk ions (calcium, nitrate, sulfate, and ammonium), submicron aerosols (fine aerosol sulfate and nitrate), and gas phase species (sulfur dioxide, carbon monoxide, ozone, and PAN).

DIAL

The Differential Absorption Lidar (DIAL) measurement system, developed by NASA Langley, measured aerosol backscattering and tropospheric ozone levels in four channels: two in the ultraviolet (UV) and one each in visible and in the infrared (IR) parts of the electromagnetic (EM) spectrum, to quantify the amount of ozone and aerosol loading, respectively (Browell et al. 2005). The vertical resolution of the DIAL measurement system was 30 m, a horizontal resolution of 2.3 km and a 10 s temporal resolution along the DC-8 flight track. The equation to calculate the aerosol scattering ratio, $R_\lambda(z)$ at a given wavelength (λ) is given by

$$R_\lambda(z) = \frac{\beta_1(z) + \beta_2(z)}{\beta_2(z)}, \quad (2.1)$$

where $\beta_1(z)$ and $\beta_2(z)$ are the backscattering coefficients ($\sim r^6/\lambda^4$) by aerosols and air molecules at altitude z , respectively.

If the size of particles is much less than the wavelength ($x=2\pi r/\lambda \ll 1$, for some of the fine mode aerosols, $r < 1 \mu\text{m}$), then the backscattering coefficient can be determined by Rayleigh scheme. Otherwise, the backscattering will be determined by the Mie theory if the size of the particles is comparable to the wavelength or greater ($x \geq 1$, for some of the fine mode aerosols and all coarse mode aerosols). Under the clear-sky conditions, the air molecules fall in the Rayleigh scattering region and their backscattering coefficient is proportional to $1/\lambda^4$. For example, the $\beta_2(z)$ at $\lambda=588 \text{ nm}$ is about 10 times greater than that at $\lambda=1064 \text{ nm}$ under the same atmospheric conditions. When the dust plumes and clouds are present, they are more probable to fall in the region

of Mie scattering. Although the backward scattering in the Mie region is weaker than that in the Rayleigh region, the backscattering coefficients $\beta_1(z)$ of dust or cloud particles are still much larger than their clear-sky background $\beta_2(z)$. Therefore, the scattering ratio $R_\lambda(z)$ at $\lambda=1064$ nm is about 10 times greater than that at $\lambda=588$ nm in the DIAL measurements. Typical scattering ratios $R_\lambda(z)$ are close to 1 for regions free of aerosol, and 2 to 10 at $\lambda=1064$ nm and 0.5 to 1 at $\lambda=588$ nm for the dust plumes (Obrecht 2008). Note that the cloud particles usually have a very large scattering ratio at both wavelengths because the backscattering coefficient is proportional to sixth power of particle size ($\sim r^6/\lambda^4$) (Frisch et al. 1994).

Nephelometer

Although DIAL measured scattering ratios can provide the location of dust plumes, difficulties arise in discerning between fine (pollution) and coarse (dust) mode aerosols in the dust plumes. Thus it is necessary to use different instrumentation to finish this task. The nephelometer is an excellent addition to the DIAL measurements, which measures optical properties of the dust plume. For the TSI Model 3563 nephelometer onboard the DC-8 aircraft, aerosol integrated light scattering coefficients at three wavelengths in the visible spectrum (450, 550, and 700 nm) were measured. For fine mode aerosols, the aerosol scattering coefficients inversely increase with wavelengths from 450 to 700 nm, but for coarse mode aerosols the aerosol scattering coefficients are nearly independent of wavelength. Therefore, for fine mode aerosols, the slope of this relationship can be given by the Angström exponent (α). The equation for calculating α is given by

$$\alpha = - [\log(\tau_{\lambda_1}/\tau_{\lambda_2}) / \log(\lambda_1/\lambda_2)], \quad (2.2)$$

where τ_{λ_1} and τ_{λ_2} are the optical depths at two given wavelengths λ_1 and λ_2 . The optical depth is proportional to the aerosol scattering ratio β_λ , therefore, the ratio of τ_{λ_1} and τ_{λ_2} is proportional to the ratio of β_{λ_1} and β_{λ_2} . Gobbi et al. (2007) pointed out that α is a good indicator of aerosol size in the solar spectrum: $\alpha > 1$ represents fine mode, submicron aerosols; $0 < \alpha < 1$ represents a mixture of coarse and fine modes; $\alpha \sim 0$ represents existing coarse, supermicron particles.

A method developed by Anderson and Ogren (1998) was used to improve the accuracy and uncertainties of nephelometer data in this study. Coarse mode aerosols of nephelometer data have two potential problems: (1) different origins (compared to fine mode aerosols) and (2) the Mie scattering effects. The scattering light of coarse mode aerosols is more concentrated into the near-forward lobe, which is usually not sensed by the nephelometer due to its design limitations (Anderson and Ogren 1998). Therefore, a delineation size between coarse and fine modes was set at 1 μm . Particle sizes larger than 1 μm (i.e., Asian dust) are considered wavelength independent (Mie scattering region due to more forward scattering) as the aerosol scattering coefficients are nearly the same at the three wavelengths used by the nephelometer. Particles smaller than 1 μm (i.e. Asian pollution) show a strong wavelength dependence and are strongly sensed by the nephelometer. These particles fall in the Mie scattering regime as they present more backward scattering. Another issue for nephelometer measurements is the biasing of sensitivity away from near-forward scattering, which is caused by the geometrical blockage of near-forward-scattering light for angles below 7° and like the previous issues,

can also be a source of great uncertainty due to the instrument design. Therefore, correction factors designed by Anderson and Ogren (1998) were applied to the nephelometer data prior to use in this study.

The correcting method of the nephelometer measurements has gone through the following steps. First, the nephelometer measurements were corrected by calibrating the instrument with gas particles since they undergo Rayleigh scattering and do not show the near-forward-scattering biases as do particles close to or greater than 1 μm (Anderson and Ogren 1998). Second, the nephelometer measurements were corrected to $0^\circ - 180^\circ$ from its original detection angles of $7^\circ - 170^\circ$. The temporal resolution of sampling averaged roughly 10 s in order to limit instrument noise. The scattering coefficients derived from nephelometer measurements are used to distinguish the coarse mode (dust) and fine (pollution) aerosols within Asian dust plumes.

Ion and Gas Chromatography

Chromatography was used to record the volatilized compounds that passed through a chemically non-reactive medium. Depending on the physical reaction to the medium (relative ease of passing through the medium), each compound will have a time of retention within the medium. The difference between gas and ion chromatography is the phase of the compounds being detected and the type of medium used, but they both operate on the same principle. Mass spectrometry involves shattering chemical species into component ions and quantifying their mass spectra. Each pattern serves as a fingerprint for a particular compound.

Dibb et al. (1996, 1997, and 2003) sampled soluble ion and fine aerosol species using ion chromatography methods, and found that the minimum detection limits for

calcium and nitrate are 5 pptv, and soluble ammonium and sulfate are 10 pptv. Fine aerosol nitrate and sulfate had the minimum detections of 3 and 6 pptv, respectively (Dibb et al. 2005). The temporal resolutions of the soluble ion and fine aerosol sampling procedure were 360 s and 88 s, respectively. The corresponding uncertainties for the measurements are as follows: ± 10 pptv for calcium, magnesium, potassium, and nitrate ions, ± 20 pptv for ammonium and sulfate ions, and up to $\pm 20\%$ for both fine aerosol nitrate and sulfate. Huey et al. (2005) sampled sulfur dioxide gas concentrations using ion chromatography and found minimum detection limit and instrument uncertainty to be ± 3 pptv and $\pm 15\%$, respectively. The sulfur dioxide concentrations were measured at a 3 s time interval. Singh et al. (2005) used gas chromatography to sample CO_2 concentrations and had instrument minimum detection limit of 1 pptv with an uncertainty of ± 2 pptv and temporal resolution of 1 s.

Diode Laser Spectrometry

Diode laser spectrometry is similar to mass spectrometry but instead of shattering the compounds, the compounds are bombarded with infrared (IR) radiation and their atoms are electronically excited to a higher energy level. This leaves behind spectra that can be used to identify various gas phase compounds. Sachse et al. (2005) sampled carbon monoxide gas concentrations via this method with an uncertainty of $\pm 2\%$ and temporal resolution of 1 s.

Chemiluminescence

Chemiluminescence involves reactions between chemical species that will produce light in a reaction chamber. This is usually done for detecting ozone with nitrogen bearing (or nitrogenous) compounds. They will react with each other to produce electromagnetic radiation in the form of visible or near visible light which is quantified to output concentrations of ozone. Avery et al. (2005) sampled tropospheric ozone using chemiluminescence with an uncertainty of $\pm 3\%$ and temporal resolution of 1 s.

Methodology

Define the area for this study

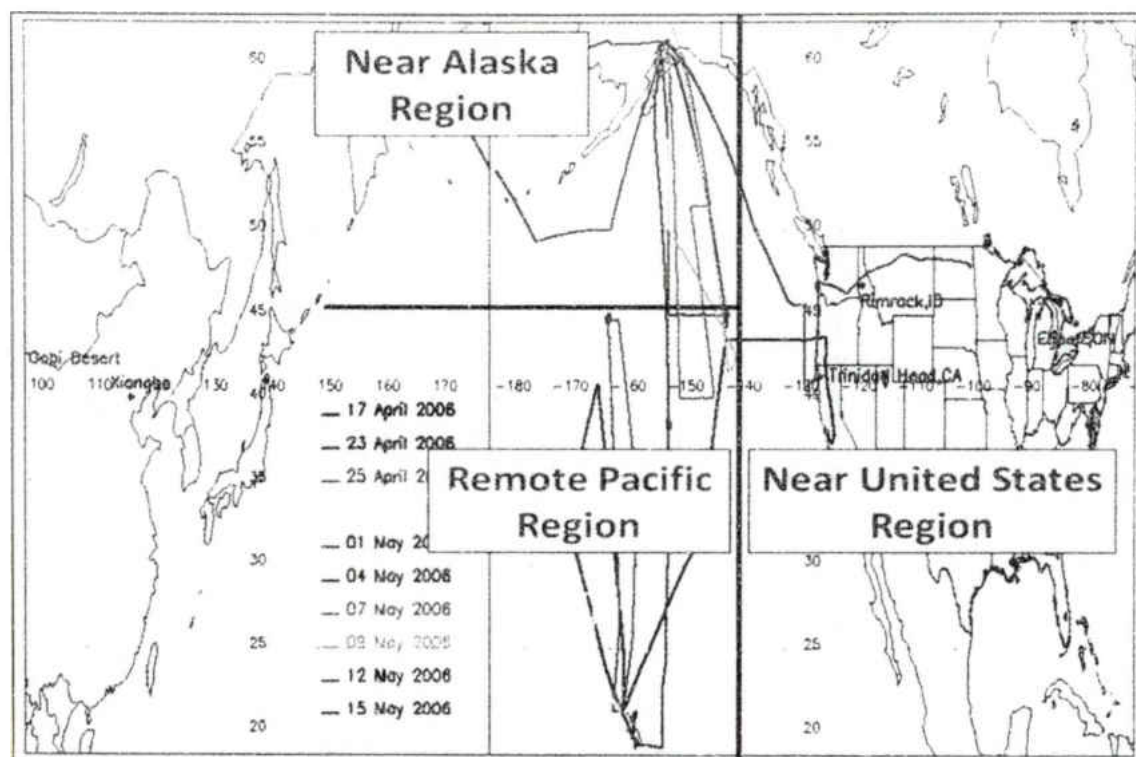


Figure 6: Summary of INTEX-B Flight Tracks with Region Bin Overlay

The INTEX-B campaign comprised ten flights conducted over the eastern Pacific between Hawaii and Alaska and terminated in the northern tier of the United States (North Dakota) as illustrated in Figure 6. The INTEX-B sampling area was separated into three regions: (1) Remote Pacific – any latitude south of 45.2°N and west of any longitude at 137°W , (2) near Alaska – any latitude north of 45.2°N and west of any longitude at 137°W , and (3) near the United States – any longitude east of 137°W . Of the ten flight tracks made during the INTEX-B campaign, the major focus of this study concerns the eight flight tracks that contain measurements from Region 1 (i.e. Remote Pacific). There are some overlaps among the three regions where flight tracks cross in and out of the pre-defined boundaries. Only the chemical and physical measurements

collected by the instruments onboard the DC-8 aircraft over the Remote Pacific region during the eight flights are analyzed in this study. Several strong dust events occurred on April 17th, April 23rd, and April 28th over the Remote Pacific region, as sampled by DC-8 aircraft and analyzed in this study.

Define the dust and pollution plume

As discussed above, the dust plumes, including fine and coarse mode aerosols, can be easily identified by using DIAL measurements of aerosol scattering ratio at 588 and 1064 nm. From DIAL measurements, we can qualitatively estimate the following: the time periods that DC-8 observed the dust/particulate phase pollution by using the aerosol scattering ratios at 588 and 1064 nm, the rough boundaries of the plumes containing both Asian dust and particulate phase pollution by using the difference of scattering ratio between the two wavelengths, and the time periods that had cloud contaminations by using the depolarization ratios. However, it is difficult to quantitatively analyze the dust plumes by using DIAL measurements alone.

Along the DC-8 flight track, if the calcium concentration is greater than 100 pptv the regions of air parcels is defined as "in plume of Asian dust". For identifying the Asian pollution, the background values of sulfur dioxide, ozone and peroxyacetyl nitrate (PAN) should be less than 100 pptv, 40 ppbv, and 0.1 ppbv, respectively (Dibb et al. 1996, 1997, and 2003; Singh et al. 2005). In other words, if the measured concentrations during the DC-8 flights are greater than the background values, then the regions or air parcels are polluted.

Methodology for Addressing the First Scientific Question

Four criteria or steps were established in this study for selecting the cases to answer the proposed first question. These criteria are (1) only the observations over remote Pacific were used, (2) DIAL aerosol scattering ratios at 588 and 1064 nm were used to determine the time periods and altitudes of the dust plumes, (3) the locations of all plumes must be in the free atmosphere in order to eliminate any sea salt contaminations and well below the tropopause to minimize the stratospheric air contaminations, and (4) the nephelometer total aerosol scattering coefficient at 450, 550, and 700 nm wavelengths were used to identify the fine and coarse model aerosols in the dust plumes.

In the previous study using INTEX-B data (Obrecht 2008), the Angström exponent (α) was used at both source (Asia) and sink regions (United States) to prove the existence of dust particles and did not, however, use the nephelometer in-situ measurements to calculate the Angström exponent during the transport processes of the dust plumes. In order to analyze the properties of dust plumes carrying mixtures of both Asian dust and pollution, Gobbi et al. (2007) proposed a method involving both spectral curvature ($\delta\alpha$) and α to track mixtures of pollution with dust. Spectral curvature is defined as the change in α over a range of three wavelengths and is useful in separating fine mode aerosols ($\delta\alpha < 0$) from mixtures ($\delta\alpha > 0$) (Gobbi et al. 2007).

The equation for calculating $\delta\alpha$ using the α measurements at the wavelengths of 450, 550, and 700 nm is as follows:

$$\delta\alpha = \alpha_{450-700} - \alpha_{550-700} \quad (2.3)$$

This equation was developed from the previous studies (cited in Gobbi et al 2007) relating $\delta\alpha$ and α to aerosol size distribution. The values used for deriving empirical relationships in these studies ranged from -1 to 1 unit ($\delta\alpha$ is a dimensionless quantity as is α). In the Gobbi et al. (2007) study, they demonstrated that spectral curvature ($\delta\alpha$) can be very close to zero under the conditions of low concentration of fine aerosols. By using the relationship between $\delta\alpha$ and α , they were able to discern situations where fine mode aerosols were dominant in a modeled dust plume from a mixture of both fine and coarse mode aerosols. They further suggested that any appreciable concentration of fine aerosol particles (Asian pollution) could affect the overall physical properties of the Asian dust plume.

Table 1 gives examples of mean Angstrom exponent values for desert and urban regions in Asia. Desert regions typically have α values less than 1 due to a stronger presence of coarse mode particles while urban areas that are dominated by fine mode pollution particles have α values greater than 1. In the case of Lanzhou (α value close to 1), this site is downwind from the Gobi desert which contributes more coarse mode dust particles to the polluted air. Coexistence of coarse and fine particles is evidenced at the polluted sites downwind of arid regions (Gobbi et al 2007).

Site Name	Ecosystem	alpha
Fukang	desert	0.99 ± 0.38
Eerduosi	desert	0.42 ± 0.41
Shapotou	desert	0.71 ± 0.29
Shanghai	urban	1.08 ± 0.24
Lanzhou	urban	0.90 ± 0.23
Beijing	urban	1.48 ± 0.56

Table 1: Annual Means and Standard Deviations of α Measured at Sites in the Chinese Sun Hazemeter Network (CSHNET)

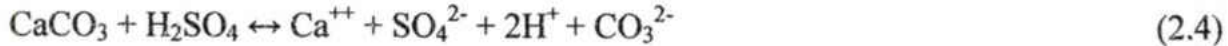
Methodology for Addressing the Second Scientific Question

The criteria and steps for selecting cases in this study utilized for answering the second question are as follows: (1) the dust plume was sampled by DC-8 in situ at least for 10 minutes in order to analyze the chemical concentrations, (2) the concentrations of chemical tracers of Asian pollution was used to identify the amount of fine and coarse mode pollution, (3) a mathematical relationship between the amounts of fine/coarse mode pollution and unreacted Asian dust in the plume was derived to quantify dominant pathways of formation of fine/coarse mode pollution in the plume. In order to address the second question, the following assumptions are made: (a) fine mode aerosol is completely soluble and contains mainly aqueous phase HNO_3 and H_2SO_4 , (b) the total soluble ion data represent both fine and coarse nitrate and sulfate aerosols, and (c) the portion of calcium ions that are not taken by both acids is synonymous with the unreacted Asian dust fraction. The mixing ratio of unreacted portion will be given by the difference of mixing ratios between calcium ion and the sum of coarse-mode sulfate and nitrate (Fig. 8).

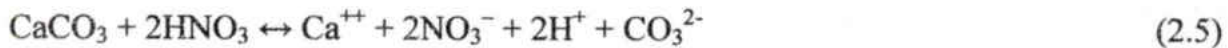
Figure 7 is a schematic diagram that shows the steps involved in pollution reacting with Asian dust. Step A represents the unreacted Asian dust particles, those are

quite often generated from desert areas with free of pollution and composed primarily of carbonates and silicates with very little natural sulfate (Jordan et al. 2003). Step B is the mixing process of particle phase Asian dust and gas phase pollution the dust plumes transport over the polluted regions, such North-eastern Asia. There is an intermediate step between Steps B and C, which demonstrates the heterogeneous reactions to convert gas phase pollution into either aqueous phase fine mode pollution or a solid coarse mode mixture of pollution and Asian dust. For example, sulfur dioxide and nitrogen dioxide can react with the calcium ions of the dust plumes to form hydrated calcium sulfate ($\text{CaSO}_4 \cdot 2\text{H}_2\text{O}$ or gypsum) and calcium nitrate ($\text{Ca}(\text{NO}_3)_2$), both soluble sulfate and nitrate species. The reaction mechanisms are given by the following expressions:

Caicium Sulfate



Calcium Nitrate



Since the bulk ion nitrate data does not account for the stoichiometric reaction in Eq. 2.5 (i.e. molar quantities of reactants and products involved in the reactions with free calcium ions to form coarse mode nitrate) it is necessary to make the adjustment when calculating the coarse mode nitrate fraction. No such correction is needed for the fine (aqueous phase) nitrate fraction. Step C shows the coexistence of both fine and coarse mode pollution within the dust plumes.

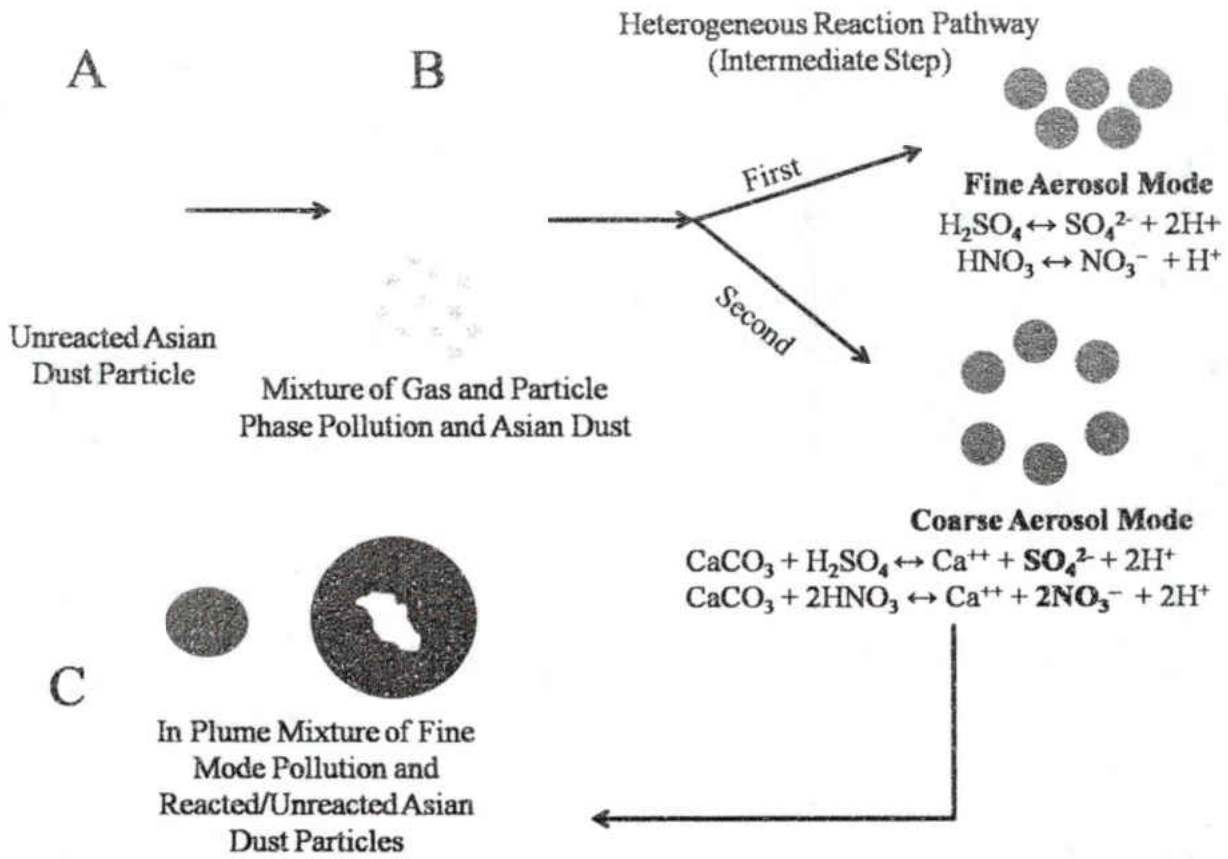


Figure 7: Mechanism for reaction of Asian dust with gas and solid phase pollution within the plume.

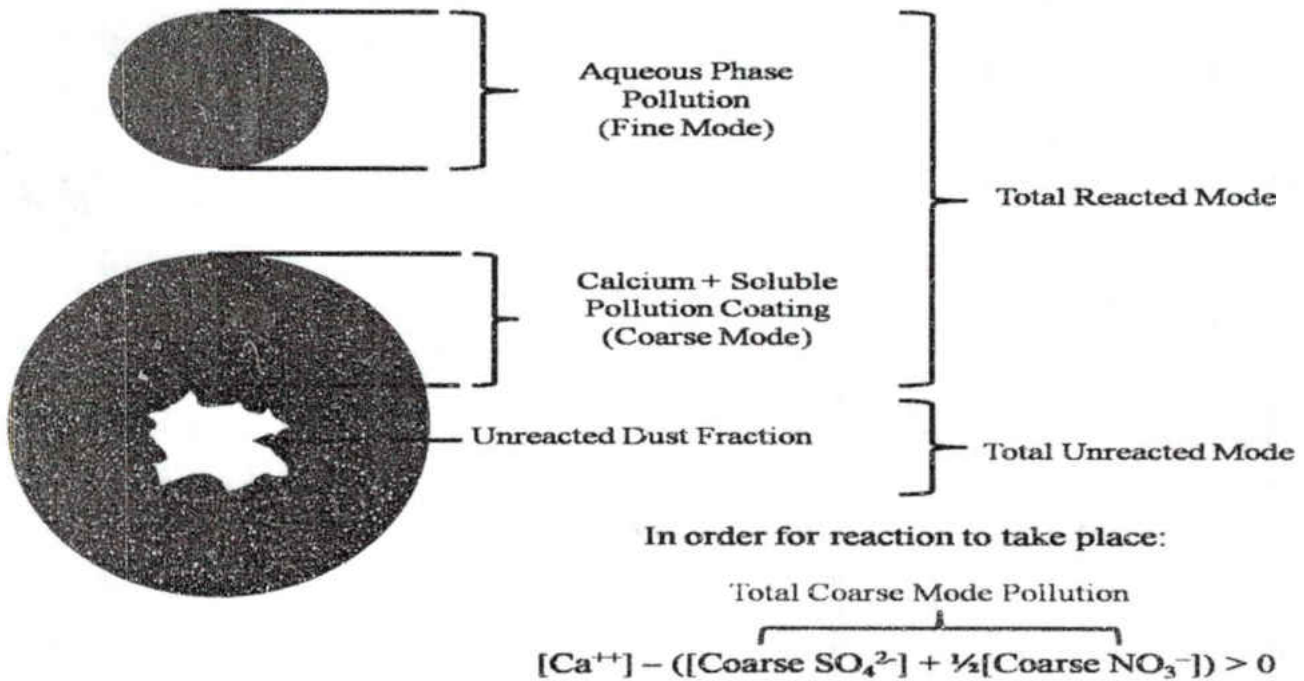


Figure 8: Description of fine mode and soluble sulfate during Step C

Ion chromatography can only measure the soluble portion of the samples collected either by Teflon filter or mist chamber on board DC-8 aircraft. From the current available data, we can only quantify total soluble mode and fine mode ion data. In order to estimate other parameters, an indirect relationship can be inferred by using the mean total soluble ion and fine mode concentrations of sulfate, nitrate and calcium. For example, the following series of expressions can be used to calculate the amount of unreacted calcium with the aqueous phase pollution (sulfate and nitrate):

$$[\text{Total Soluble Nitrate}] = [\text{Total Coarse Nitrate}] + [\text{Total Fine Nitrate}] \quad (2.6a)$$

$$[\text{Total Coarse Nitrate}] = ([\text{Total Soluble Nitrate}] - [\text{Total Fine Nitrate}]) \quad (2.6b)$$

$$[\text{Total Soluble Sulfate}] = [\text{Total Coarse Sulfate}] + [\text{Total Fine Sulfate}] \quad (2.6c)$$

$$[\text{Total Coarse Sulfate}] = [\text{Total Soluble Sulfate}] - [\text{Total Fine Sulfate}] \quad (2.6d)$$

$$[\text{Total Fine Mode associated with Calcium ions}] = \frac{1}{2}[\text{Total Fine Nitrate}] + [\text{Total Fine Sulfate}] \quad (2.6e)$$

After combining Eqs. 2.6b, 2.6d, and 2.6e, the Total Soluble Mode is given by:

$$[\text{Total Soluble Mode}] = [\text{Total Coarse Mode}] + [\text{Total Fine Mode}] \quad (2.7)$$

Eq. 2.7 is used to estimate the coarse mode (soluble sulfate/nitrate coating) concentrations if the total soluble mode and fine mode ion data can be directly measured by DC-8 aircraft. The unreacted calcium mode can then be derived by subtracting total

soluble coarse mode (given by Eq. 2.7) from the total calcium mode in the following equation:

$$[\text{Unreacted Calcium}] = [\text{Total Soluble Calcium}] - [\text{Total Coarse Mode Calcium associated with acidic ions}] \quad (2.8)$$

where

$$[\text{Total Soluble Calcium}] - [\text{Total Coarse Mode}] > 0 \quad (2.9)$$

The magnitude of the difference between the calcium and soluble coarse mode pollution mixing ratios is directly related to the amount of unreacted Asian dust. The closer the expression given in Eq. 2.9 is to zero, the more complete the gas to particulate reaction that generates the soluble coating on the dust particle. In the dust-free cases, these relationships cannot be used due to lack of reaction sites for coarse mode pollution to form (Fig. 8). In essence, a negative value will result which signifies an absence or deficit of calcium ions or surplus of aqueous phase nitrate and sulfate ions; neither of which can be inferred by the given data sets.

Reactions involving ammonium with nitrate and sulfate occur in fine mode more often than in coarse mode. Though neutralization reactions between ammonium and nitrate/sulfate can take place on the surfaces of the Asian dust particles, the fine mode pathway is more favored (Eq. 1.3) (Jordan et. al. 2003). The main reason is the difficulty in reacting ammonium ions with calcium ions on the surface of the Asian dust particles as

they both behave as bases. The reaction between ammonium and calcium in the aqueous phase can produce an insoluble calcium hydroxide fraction that will be unavailable to react with either nitrate or sulfate.

CHAPTER III

RESULTS

The First Scientific Question

Figures 9-11 show the aerosol scattering ratios at 1064 nm as measured by DIAL. By inspecting DIAL plots for the selected eight flight tracks, the dust/particulate phase pollution plume, clouds, and dust-free regions and altitudes can be determined by examining the range of the values of scattering ratios. The aerosol scattering ratios between 2 and 10 (yellow to light orange) may account for the observed dust/particulate phase pollution plume, more than 50 are for most of clouds, and between 10 and 50 may be the strong dust events or marine boundary layer clouds. For the marine boundary layer clouds, the scattering ratios ranged from 10 to 50, but the depolarization ratio spherical cloud droplets are quite different from the non-spherical dust particles. In order to reduce the marine boundary layer cloud contamination, the dust plumes selected in this study were well above the boundary layer (> 2 km).

The depolarization ratio is another DIAL measurement, which is defined as the ratio of the backscattered signals of the perpendicular to the parallel polarization of backscattered light, as measured with the emitted linear polarized laser. For the spherical particles, the depolarization ratios are normally less than 10%. Because the dust particles are both in the solid phase and highly non-spherical, their depolarization ratios should be

more than 10%, but less than those for cirrus clouds (~30-50% depending on ice particle size distributions, Sassen 1991).

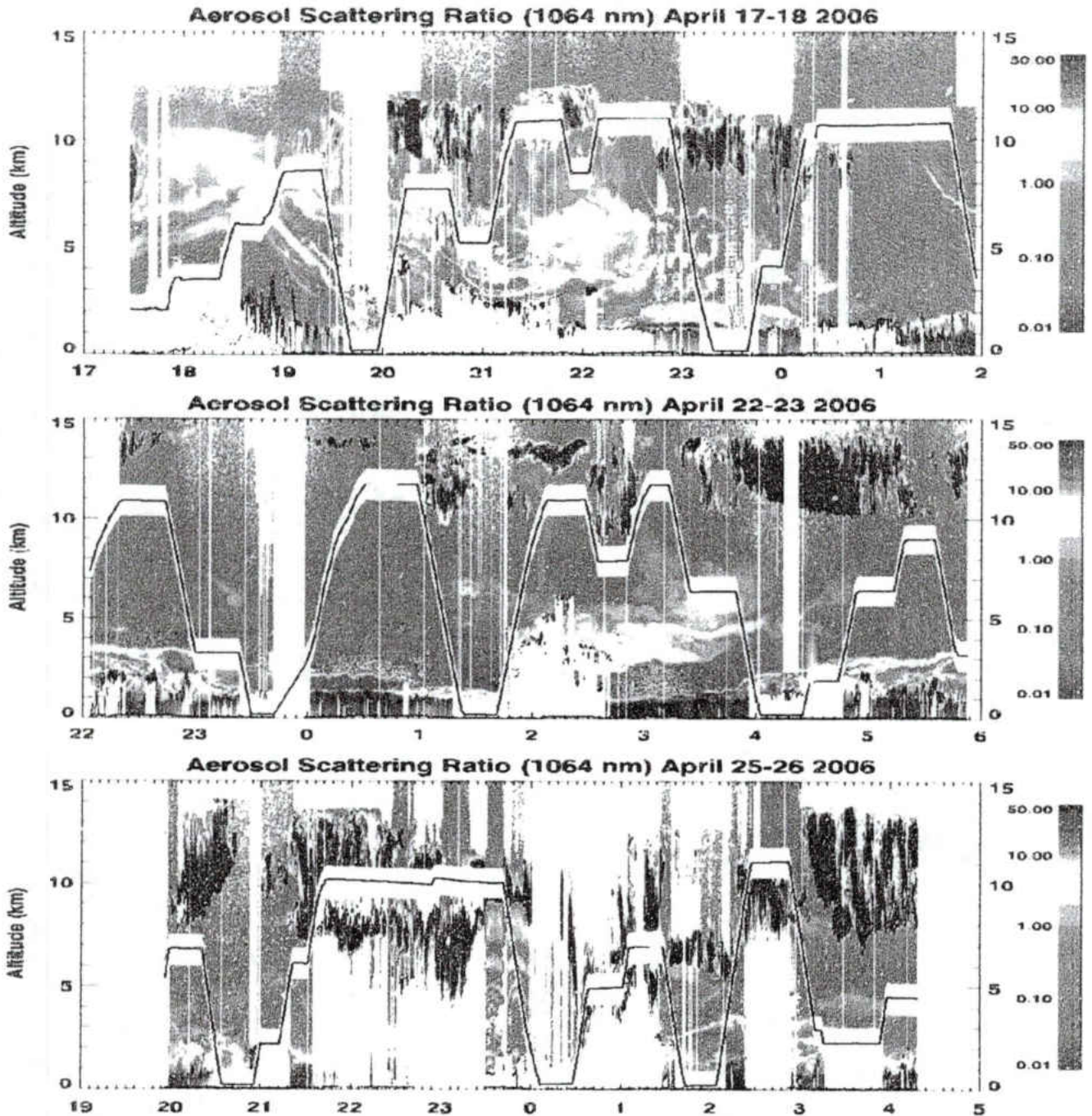


Figure 9: DIAL Plots for April 17, April 23, and April 25

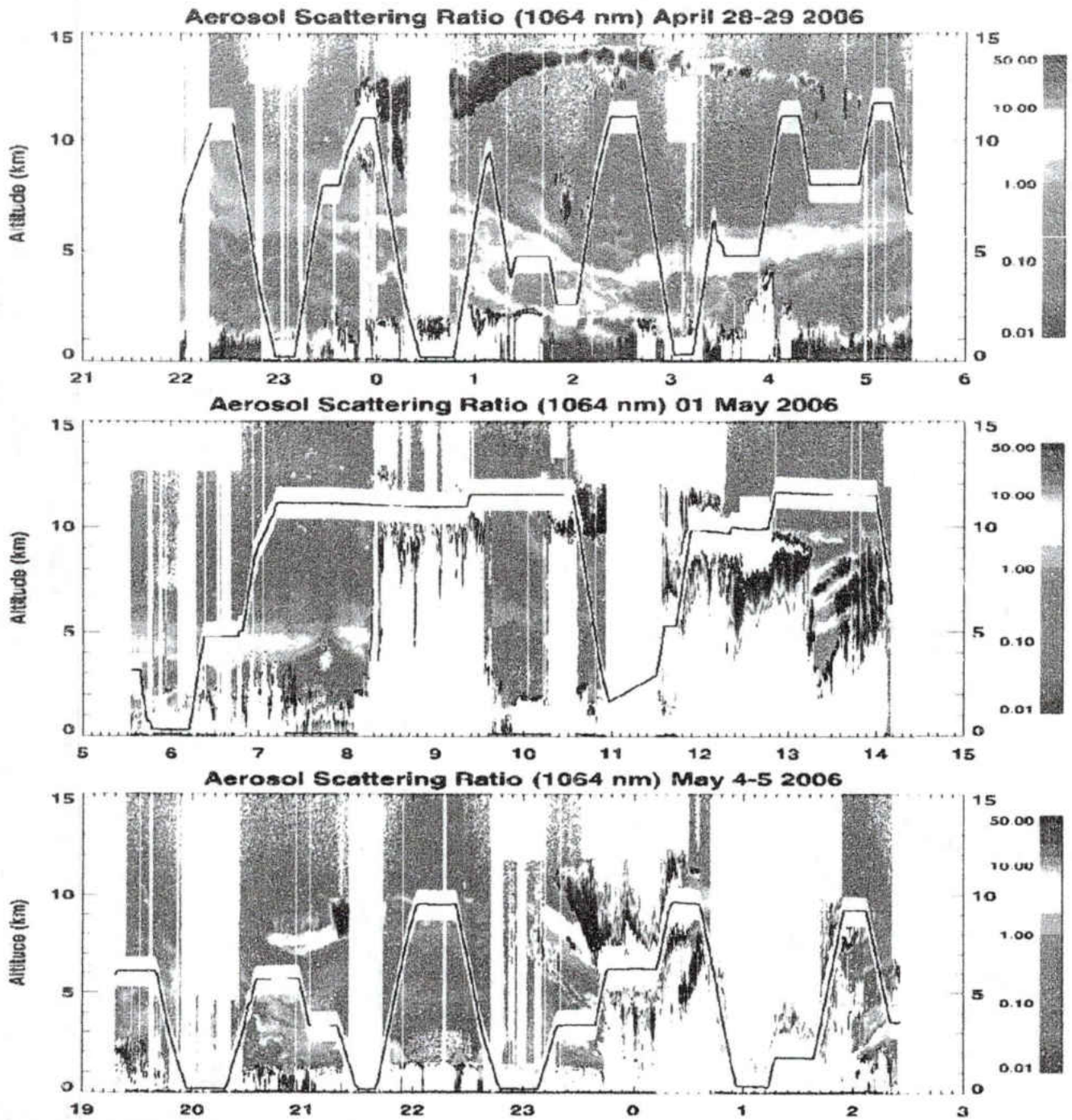
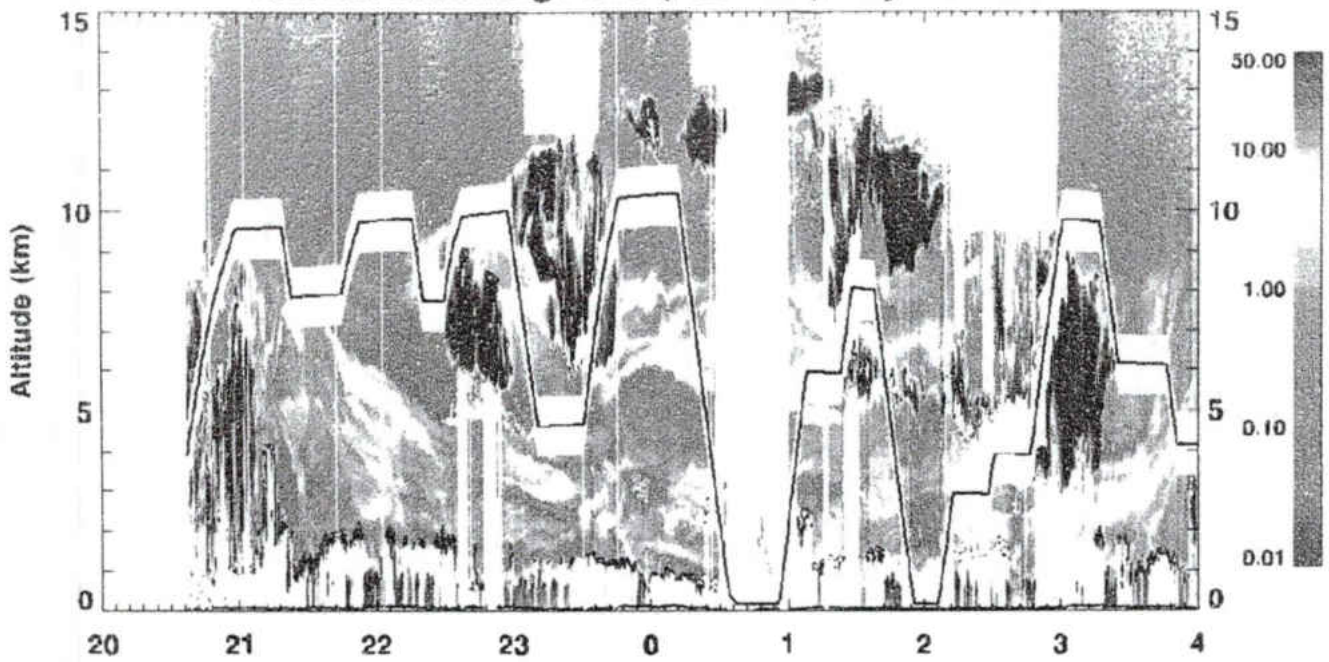


Figure 10: DIAL Plots for April 28, May 1 and May 4

Aerosol Scattering Ratio (1064 nm) May 7-8 2006



Aerosol Scattering Ratio (1064 nm) May 9-10 2006

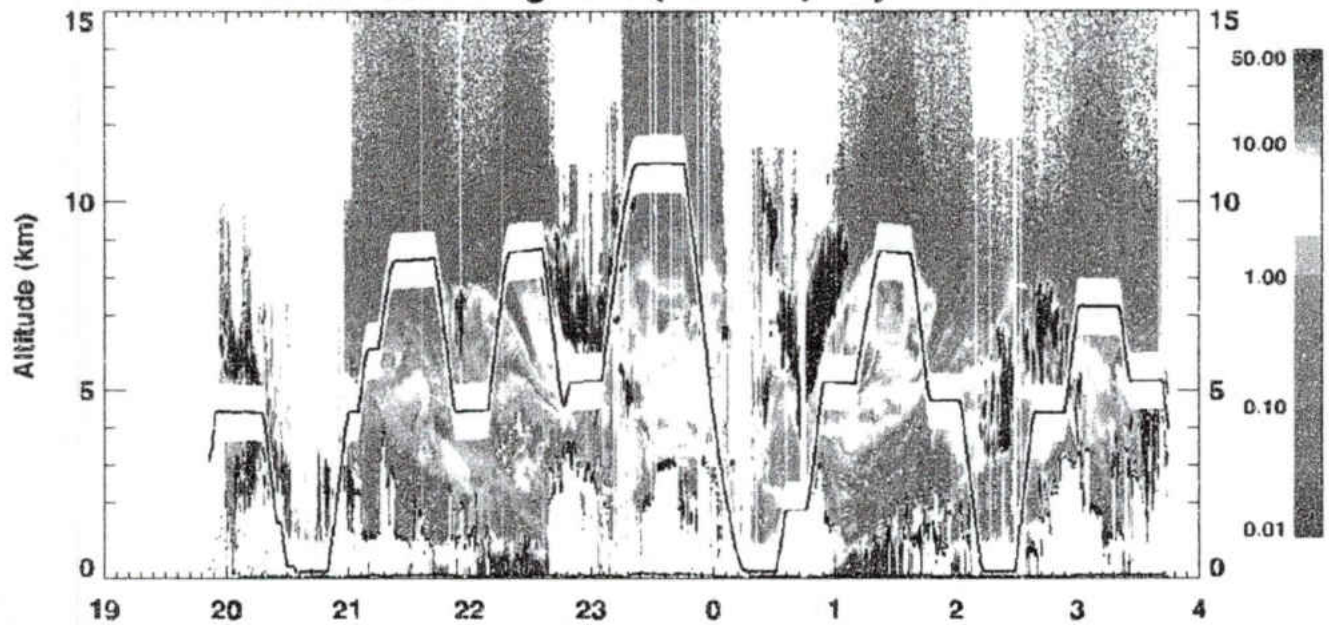


Figure 11: DIAL Plots for May 7 and May 9

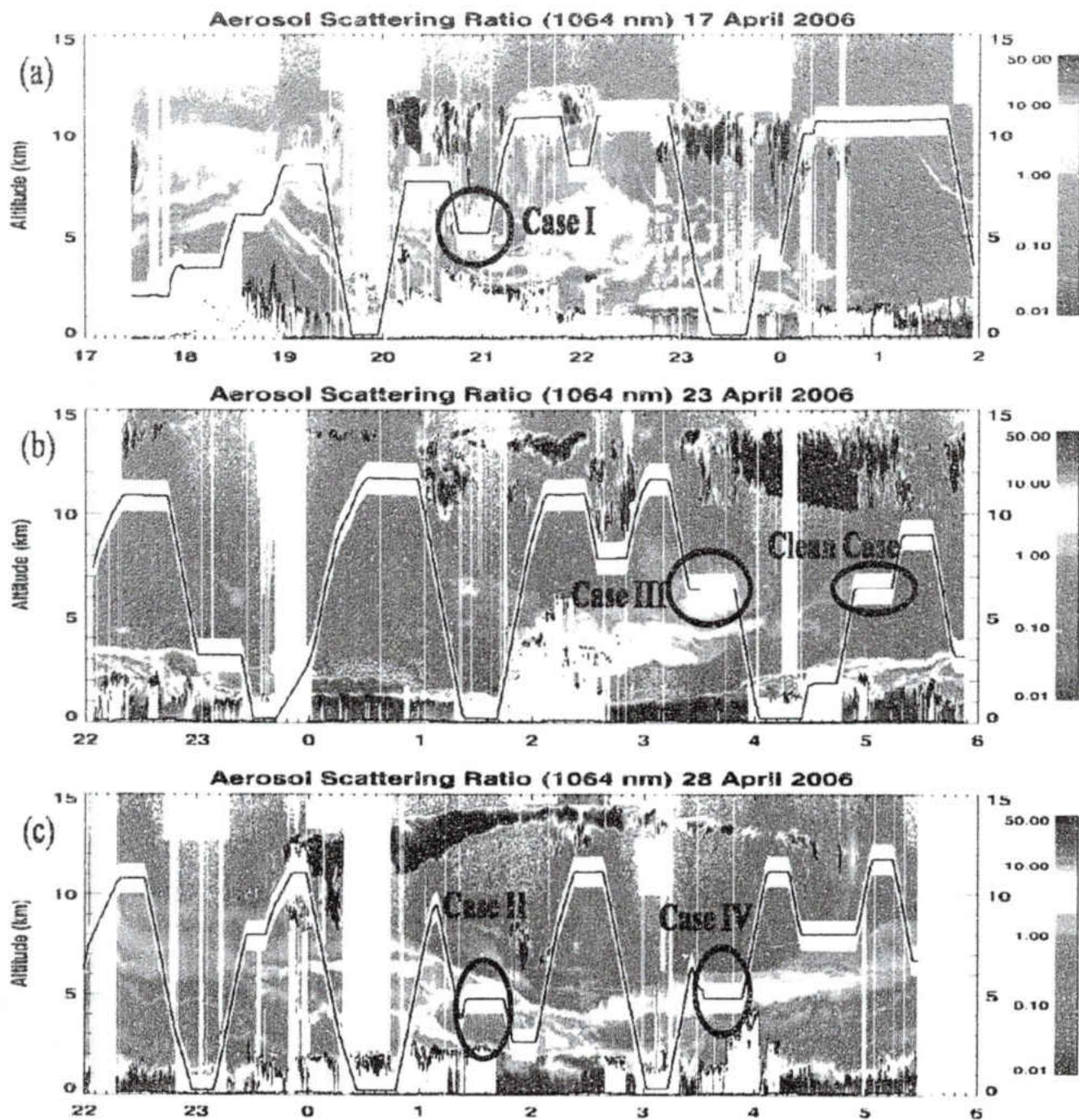


Figure 12: DIAL Backscattering Ratio Plots for the Four “In Plume” Case Studies and the Clean Case

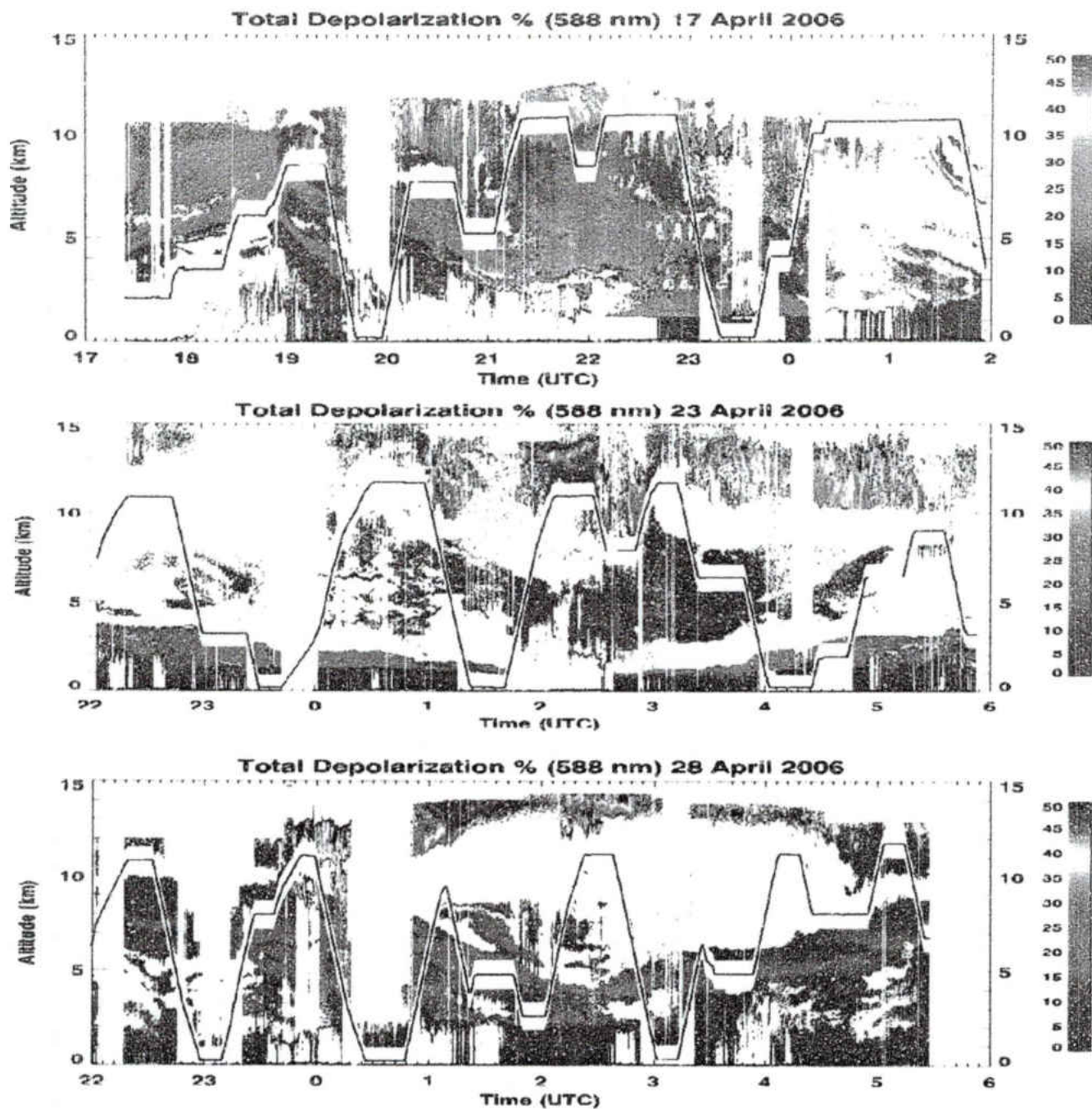


Figure 13: Depolarization Plots during the case study time dates and time intervals

After carefully examining the regions by using the third and fourth criteria listed in Chapter II, the four time periods that met the requirement for further analysis during entire INTEX-B experiments were selected and indicated by the black circles in Figure 12. The selected four cases used for the detailed analysis are: the Case I, 20.5-21.5 UTC

on April 17, 2006; the Case II 1-2 UTC on April 29, 2006; the Case III 3-4 UTC on April 24, 2006; and the Case IV, 3-4 UTC April 29, 2006. All four cases have nearly the same vertical altitude from 3 to 7 km. Figure 13 shows the depolarization ratios for the selected four cases with the corresponding values of 20-30% for the dust plumes at 1064 nm. For 3 out of the 4 cases, the depolarization ratios fall into this range which leaves only Case III as having a much lower depolarization ratio. This may be a possible case for a particulate pollution plume with little dust loading.

As discussed above, the time periods and altitudes of dust plumes can be easily identified by using DIAL measurements of aerosol scattering ratio at 588 and 1064 nm. However, it is difficult to quantitatively analyze the dust plumes by using the DIAL measurements, especially for discerning the fine and coarse mode aerosols in the dust plumes. Therefore, it is necessary to use the nephelometer data to do further study.

Nephelometer data in conjunction with the technique developed by Gobbi et al. (2007) are utilized to verify which mode (fine or coarse) aerosols dominated in the selected four dust plumes. Scattering ratios and Angström exponent values are used as proxies for both Asian dust and pollution. Figures 14 and 15 show the observations taken from the nephelometer, mist chamber, and Teflon filter for the four selected dust plumes. A brief summary of these observations for each case is discussed as follows.

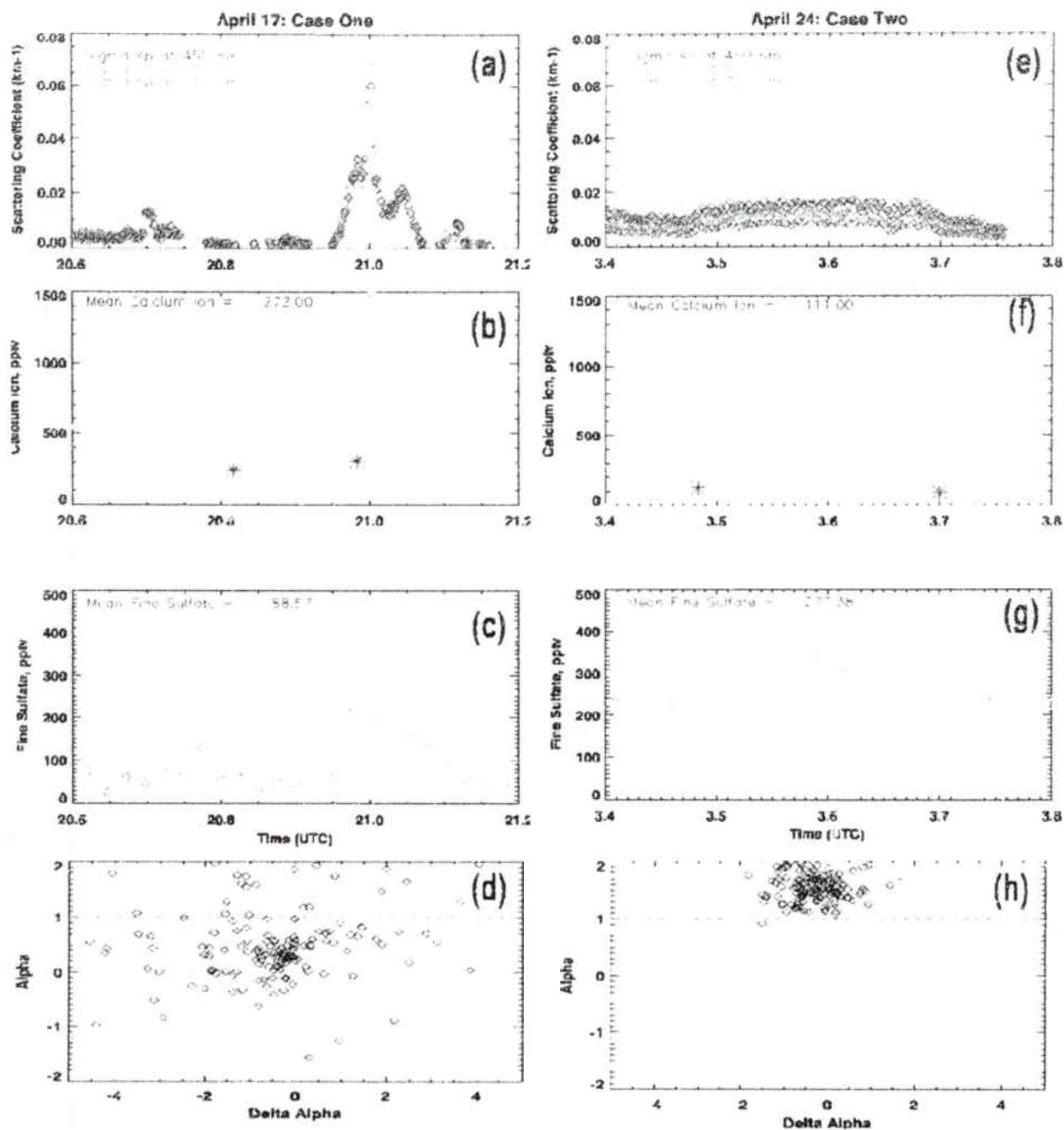


Figure 14: (a) The scattering coefficients at three wavelengths (450, 550, and 700 nm), (b) calcium ion concentration, (c) fine sulfate concentration, and (d) the Angström exponent α observed by the TSI Model 3563 nephelometer onboard the DC-8 aircraft on April 17, 2006. For the April 24 case, (e-h) are the same as (a-d).

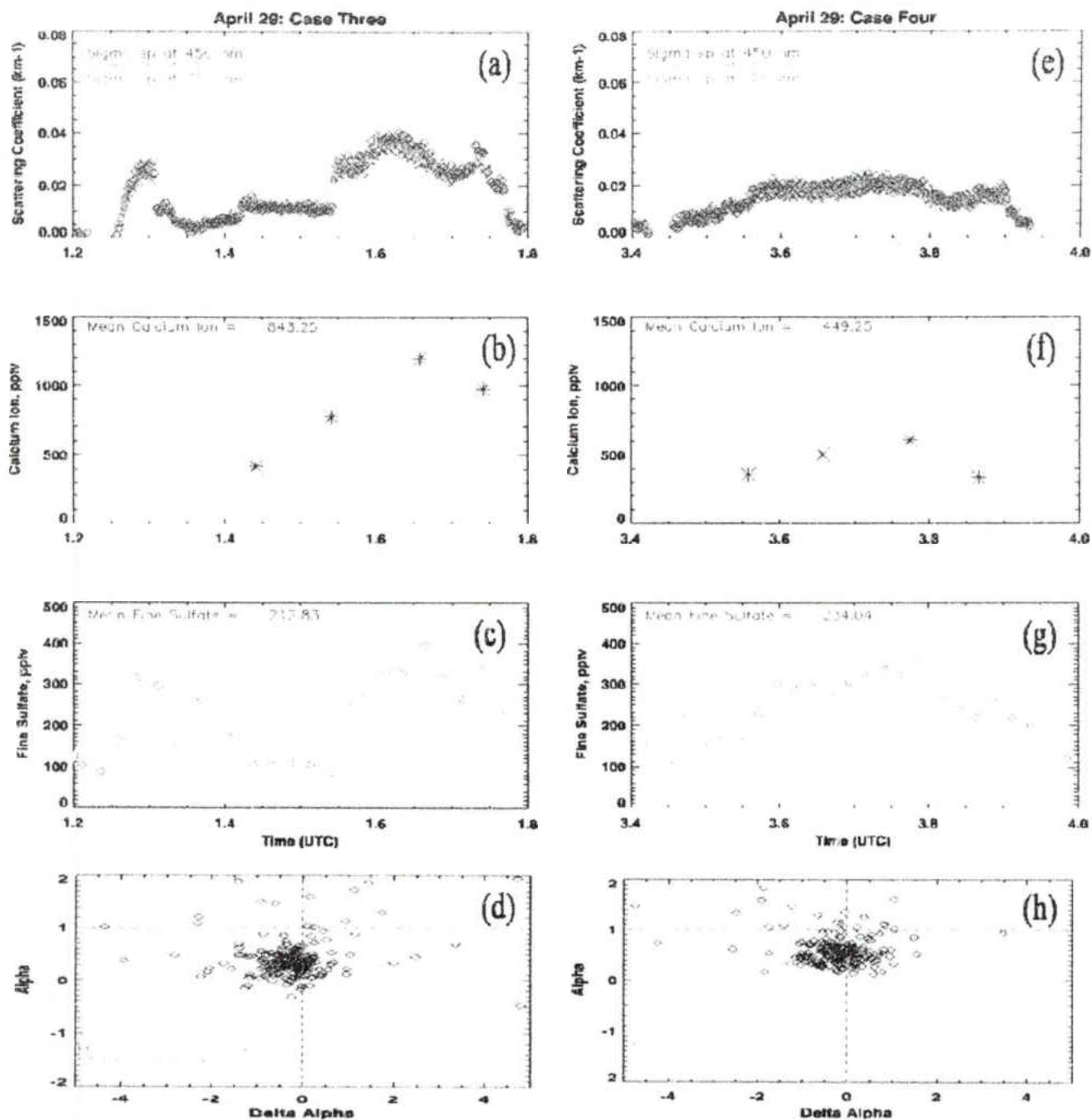


Figure 15: Two April 29 cases. (a) The scattering coefficients at three wavelengths (450, 550, and 700 nm), (b) calcium ion concentration, (c) fine sulfate concentration, and (d) the Angström exponent α observed by the TSI Model 3563 nephelometer onboard the DC-8 aircraft. (e-h) are the same as (a-d)

Case I: April 17, 2006

The spectral data show a weak wavelength dependence of scattering coefficient values at three different wavelengths (Fig. 14a) until a peak at 2100 UTC appears where the wavelength dependence increases suddenly. Immediately after the peak, the dependence becomes negligible. The mean calcium ion concentration is about 272 pptv (Figure 14b), which suggests a moderate amount of dust within the plume. The mean fine mode sulfate concentration is 89 pptv (Figure 14c), which is considered below the polluted levels. Corresponding to the spike in the scattering coefficients, there is also a sharp increase in fine mode sulfate at the identical time where the values rise to over 200 pptv. Similarly to the spectral data, fine mode sulfate concentration decreases to background (less than 100 pptv) values after the spike. Figure 14d shows that the mean (and standard deviation) Angström exponent (α) is 0.46 ± 0.63 , which suggests an abundance of coarse mode particles existed in the plume. Although a negative $\delta\alpha$ mean value of -0.49 is indicative of a strong fine mode aerosol in the plume as given by Gobbi et al. (2007), the Angström exponent and calcium ion data indicate that the coarse mode aerosols are dominant in this case.

Case II: April 24, 2006

Figure 14e shows a strong wavelength dependence of the scattering coefficients at three wavelengths. The scattering coefficients at the shorter wavelength ($\lambda=450$ nm) are consistently larger than those at the higher wavelength ($\lambda=700$ nm) because the backward scattering coefficients decreases with increasing the wavelength as the fine mode aerosols exhibiting in the plume. Note that the scattering coefficients decreased with the increasing wavelengths as shown in Fig. 14e, that is, the observational data demonstrated

the existing the fine mode within the plume. The low mean calcium ion concentration, as shown in Fig. 14f (111 pptv, slightly above the background value) and the high fine mode sulfate concentration (277 pptv) also indicate that the fine mode aerosols are dominant in this case. The averaged Angström exponent α (Fig. 14h) is 1.53 ± 0.23 and the $\delta\alpha$ values lie mostly in the negative range with a mean value of -0.31, which further proved the above discussions that Asian pollution (or fine mode aerosols) dominated in the Case II.

Cases III and IV: April 29, 2006

Cases III and IV (Fig. 15) were observed on the same day, April 29, but at different time periods. Their scattering coefficients and concentrations fell between those from Case I and Case II (i.e., the mixture of coarse and fine mode aerosols in the dust plumes). For example, the scattering coefficients at the three wavelengths are nearly the same during the period 1.3-1.54 UTC when the fine mode sulfate concentration is low (< 200 pptv). After that, the sharp peaks occurred for both the scattering coefficients and fine mode sulfate concentrations where the scattering coefficients and their differences at three wavelengths strongly correlate with the fine mode sulfate concentrations. In other words, both scattering coefficient values and their differences strongly increased with the increased the fine mode sulfate concentrations (~ 300-400 pptv) as demonstrated during the period of 1.54-1.77 UTC. However, the differences are not so obvious as those in the Case II because the calcium ion concentration (~ 1000 pptv) in Case III is much higher than that (~ 111 pptv) in the Case II. Therefore, the scattering coefficients are dominated by the mixture of coarse and fine mode aerosols in the Case III, especially during the period of 1.54-1.77 UTC when both Calcium ion and fine mode sulfate concentrations are high.

Discussion

To further confirm that the four selected cases originated in Asia, the back trajectory model known as the **Hybrid Single Particle Lagrangian Integrated Trajectory Model (HYSPLIT)** was used in this study. As mentioned above, all the selected four cases had similar altitudes from 3 to 7 km, thus the outputs of the back trajectory model were selected at representative heights of 3000, 5000, and 7000 m in the central part of the plumes. These heights represent the mean depth from top to bottom of the plume with 5000 meters being the height of the “center” of the plume. The time interval of back trajectory model is 6 hours.

Figures 17 through 20 show the back-trajectory analysis of all the selected four cases. Key points describing the similarities and differences from the model output include: (a) for Cases I and III, the dust plumes originated from the Gobi desert, and (b) for Cases II and IV, the dust plumes passed through the Tibetan plateau. The transport time of dust plumes for the four cases in order are around 7.5, 3, 5, and 7 days, respectively, to reach the remote Pacific regions where the dust plumes were observed by the DC-8 aircraft. However, the transport time was only approximated because the measurements were not taken at the same location. From previous studies, the dust plumes normally take, on average, seven to ten days to move out of the Gobi desert area to the United States. Therefore, the model outputs are 240 hours in duration in order to explore all possible sources of the air masses.

For Case I, the center height of dust plumes is around 5 km, ranging from 3 to 7 km. From the back trajectory analysis, the green line in Figure 17 did not pass through central and southern China (the highly polluted area), and thus, did not pick up much

urban pollution. The blue and red lines originated from the Gobi desert area and did not pass the highly polluted area. This especially held true for the blue line where the DC-8 sampled high calcium and low fine sulfate concentrations at an altitude of 5 km. For Case II, the plume was located around 5-7 km, and sampled by DC-8 at roughly 7 km. The back trajectory showed that the green and blue lines originated from the Tibetan plateau and did pass through highly polluted areas. Therefore, the outputs of back trajectory model did support the findings from DC-8 measurements in Cases I and II.

For Cases III and IV, the green and blue lines originated from central China, and the data suggested a possible scenario of air masses containing dust plumes that were lifted above the boundary layer and passed through many urban areas. These areas may possibly carry much higher pollution during their transport than in Case I as will be discussed in the next chapter that explains the chemical concentration of the pollution.

Trajectories that come from different regions but cross paths over either the Gobi desert or Tibet plateau are also scrutinized in order to see how pollution and dust can mingle at various points during their transpacific transport processes. If dust plumes are capable of carrying pollution inside them, then the calcium concentration should correlate well with pollution.

NOAA HYSPLIT MODEL
 Backward trajectories ending at 2100 UTC 17 Apr 06
 GDAS Meteorological Data

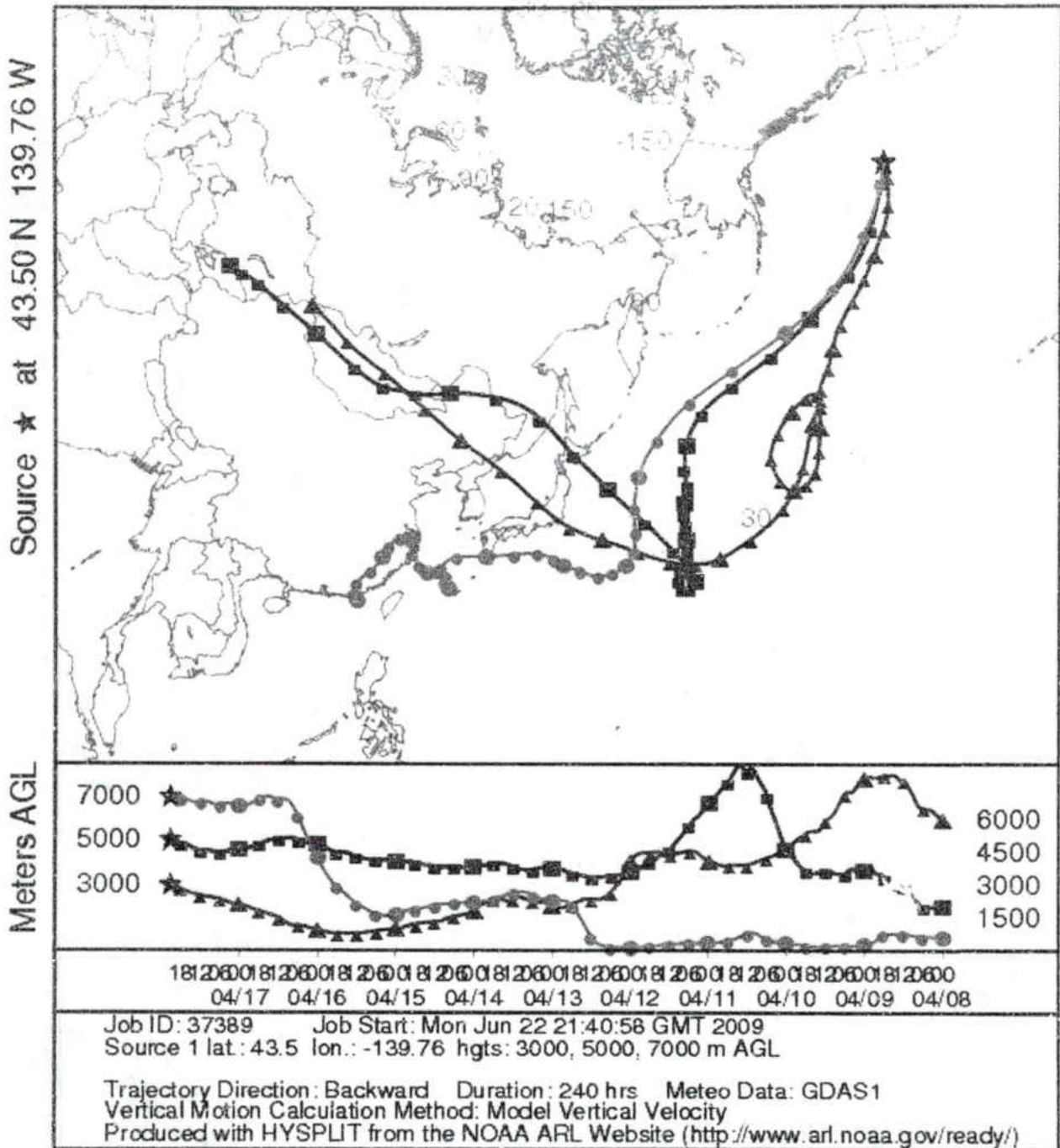


Figure 16: HYSPLIT Backward Trajectory Plot for Case I

NOAA HYSPLIT MODEL
 Backward trajectories ending at 0300 UTC 24 Apr 06
 GDAS Meteorological Data

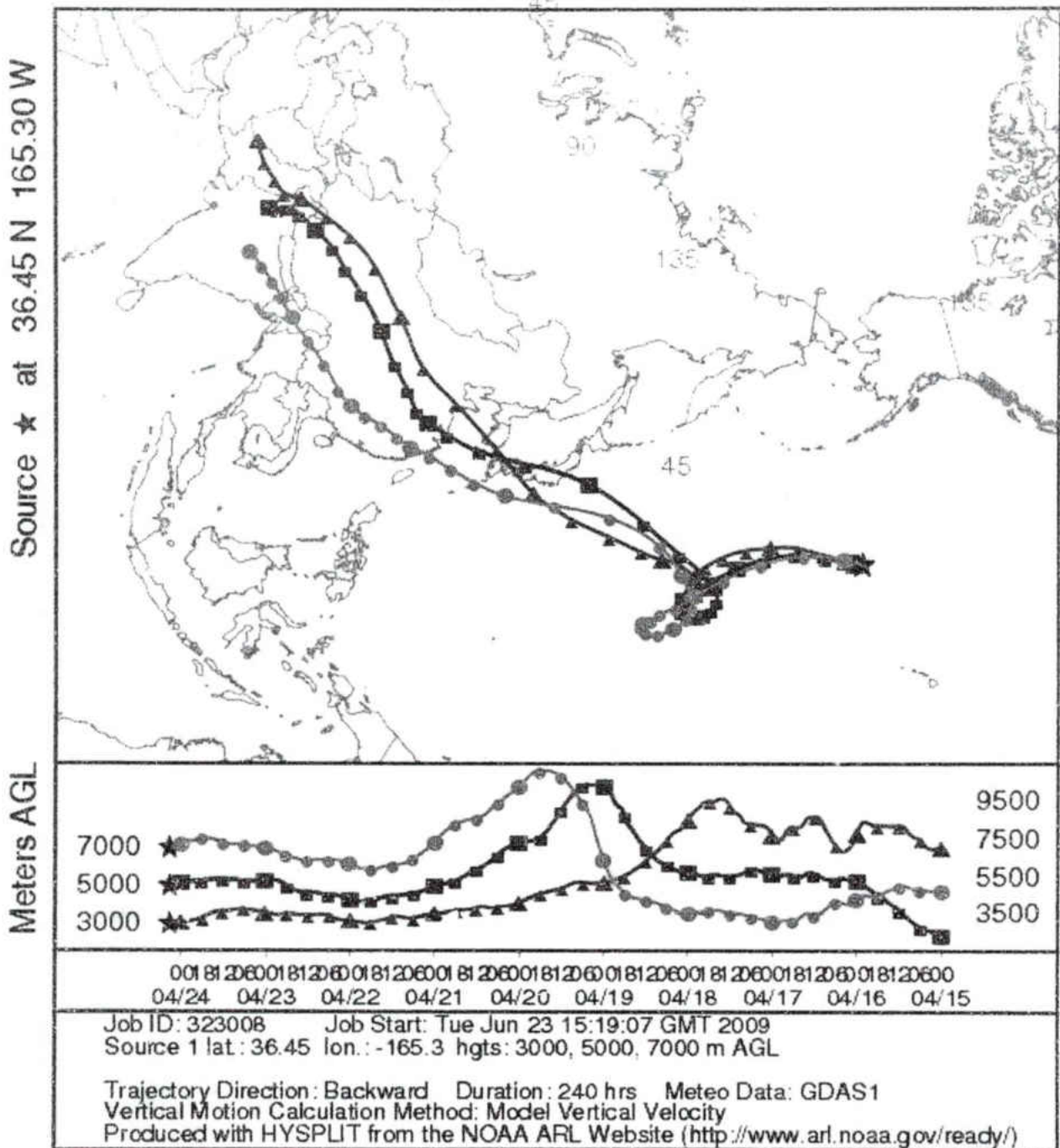


Figure 17: HYSPLIT Backward Trajectory Plot for Case II

NOAA HYSPLIT MODEL
 Backward trajectories ending at 0200 UTC 29 Apr 06
 GDAS Meteorological Data

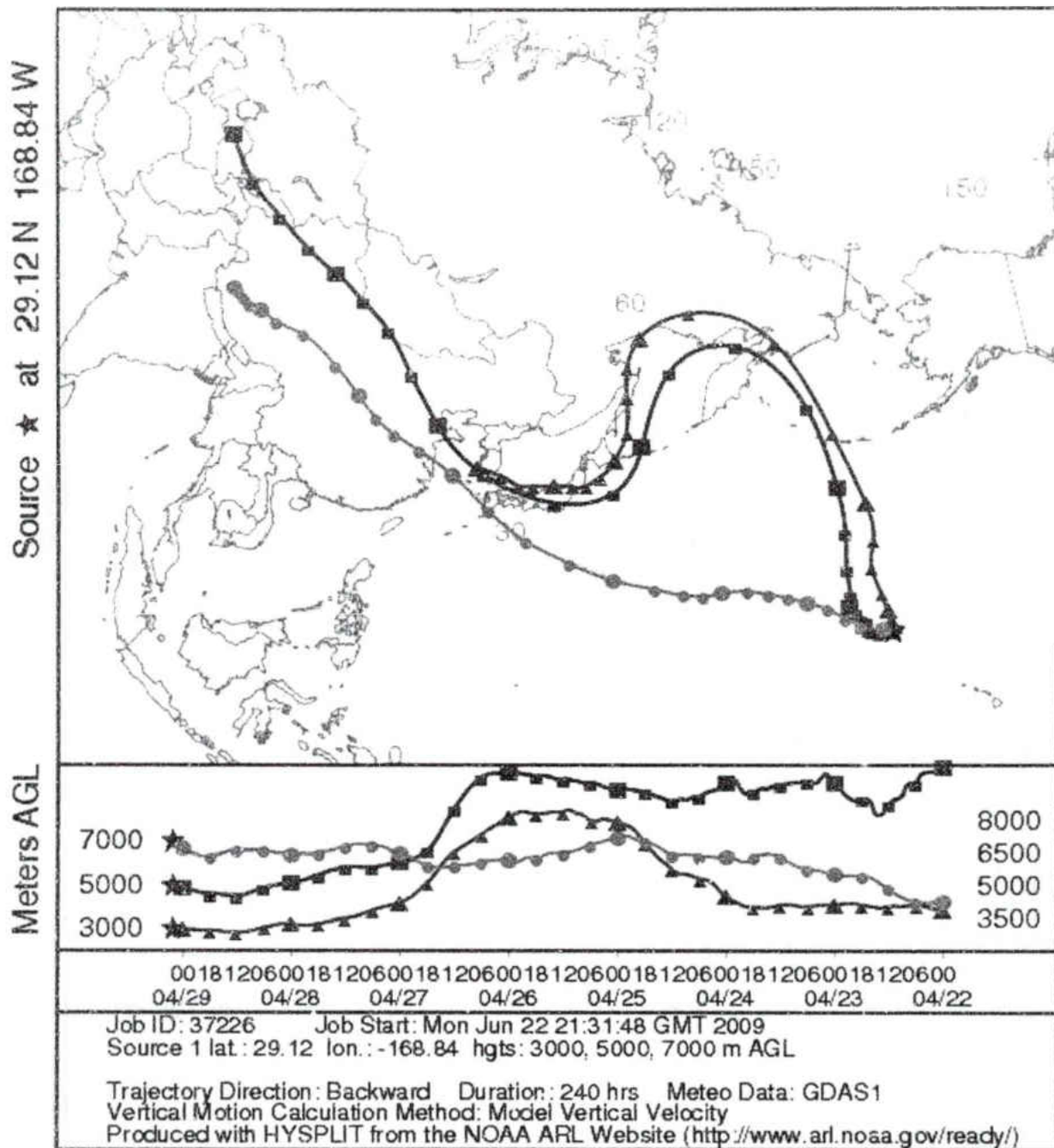


Figure 18: HYSPLIT Backward Trajectory Plot for Case III

NOAA HYSPLIT MODEL
 Backward trajectories ending at 0400 UTC 29 Apr 06
 GDAS Meteorological Data

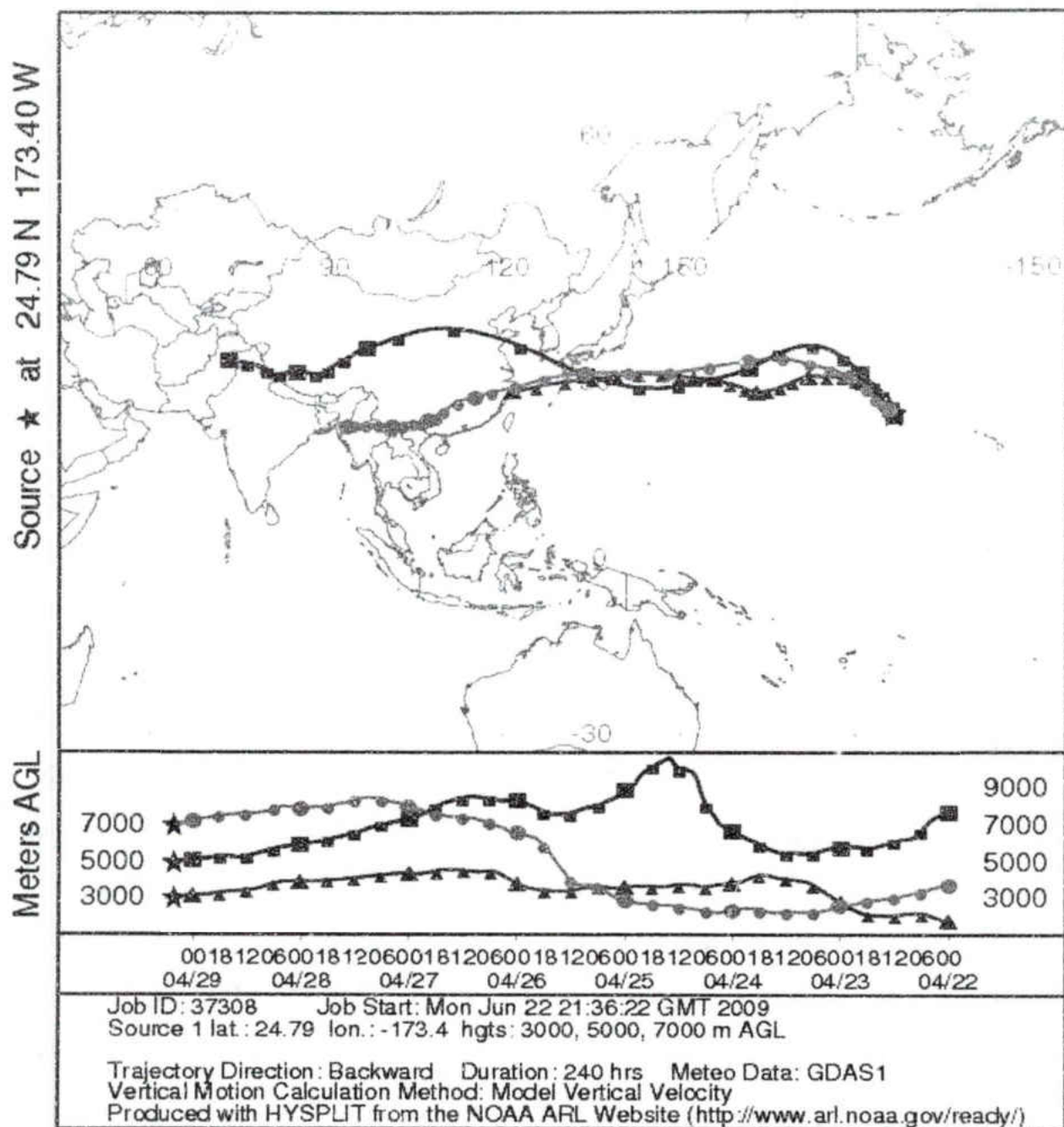


Figure 19: HYSPLIT Backward Trajectory Plot for Case IV

Table 2 gives a brief summary of the chemical and physical properties of the selected four dust plumes. The aerosol scattering coefficients for Case I had the weakest wavelength dependence, and the fine mode sulfate concentration was also the lowest

among all four cases. Though the calcium concentration was moderately elevated compared to background dust loading, this case carried much less pollution than the other three cases. From the back trajectory analysis, the blue and red lines passed through the Gobi desert area and did not pass the highly polluted area, which strongly supports the findings from DC-8 measurements for Case I: the coarse mode dominant. The aerosol scattering coefficients for Case II had the strongest wavelength dependence, and the fine mode sulfate concentration was also highest among all 4 cases. The Angström exponent (mean $\alpha > 1$) for this case suggested that the dust plume was dominated by pollution, which was further proved by back trajectory analysis. For Cases III and IV, their scattering coefficients and chemical concentrations fell between those found in Case I and Case II (i.e. the mixture of coarse and fine mode aerosols in these two dust plumes as supported by the back trajectory analysis).

	Mean [Ca ⁺⁺] (pptv)	σ (pptv)	Mean [Fine SO ₄ ²⁻] (pptv)	σ (pptv)	Mean α	σ	Mean $\delta\alpha$	σ
Case I	272	44	89	57	0.46	0.63	-0.49	1.61
Case II	111	24	277	43	1.53	0.23	-0.31	0.63
Case III	843	304	213	98	0.40	0.36	-0.25	0.97
Case IV	449	126	234	71	0.60	0.29	-0.23	0.89

Table 2: Summary of Chemical and Physical Properties of the Four Cases and Their Uncertainties as Given by Standard Deviations (σ)

Notice that aerosol scattering coefficients and the concentrations of fine mode sulfate changed over time along the flight track as the aircraft passed through the dust plume. During the case studies, we found both uniform and non-uniform variations in the two concentrations at the same time intervals may infer the degree of mixing between Asian dust and pollution during transport. Figure 21 illustrates a visual depiction of what may be occurring in these cases. It should also be noted that the spectral curvature values were negative in all four cases. The Gobbi et al. (2007) technique may not be capable of discerning between pure coarse and fine modes. It can only differentiate between fine mode dominance and a mixture of coarse and fine modes due to the negligible wavelength dependence of coarse mode particles. Negative values in these cases may suggest that the fine mode pollution does dominate the microphysical properties of the mixture of Asian dust and pollution plume. This may be due to the strong wavelength dependence as exhibited by fine mode aerosols compared to the near negligible dependence with coarse mode aerosols and the sensitivity of the nephelometer that measures the scattering coefficients.

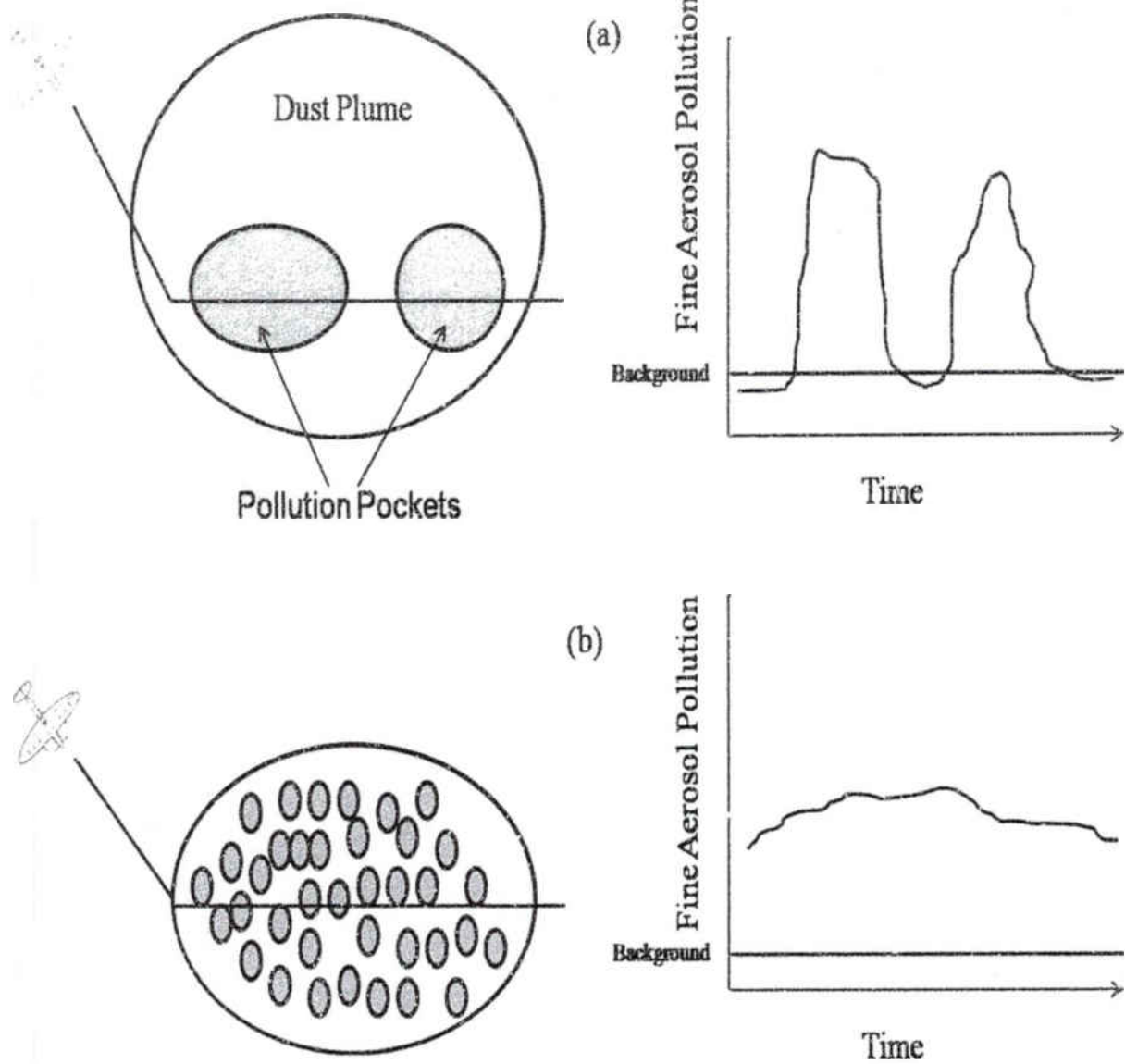


Figure 20: Depiction of a Flight Track Passing Through a Poorly Mixed Plume (a) and Well Mixed Plume (b) and the Corresponding Fine Aerosol Data over Time

The Second Scientific Question

Clean Case

Using the DIAL plot (Fig. 12b) a dust free case has been picked up, which was located almost at the same altitude as in Case III. The clean area had mean calcium, sulfate ion and nitrate ion concentrations of 30.50, 53, and 23 pptv, respectively. These values are well below the in plume threshold but above detection limits. This contrasts with the mean fine aerosol sulfate and nitrate concentrations which are 135 and 75.75 pptv, respectively. The area has aqueous mode pollution but hardly any dust so any generation of coarse mode pollution is either negligible or non-existent.

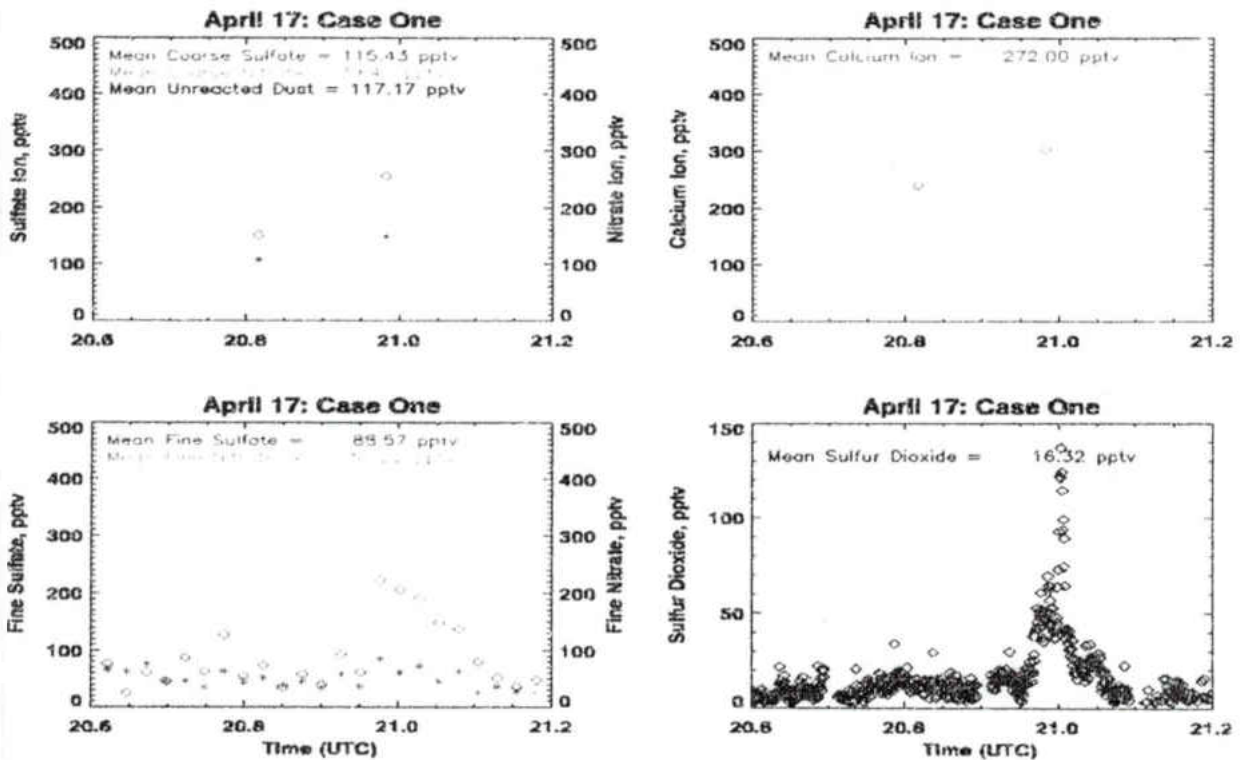


Figure 21: April 17 Case

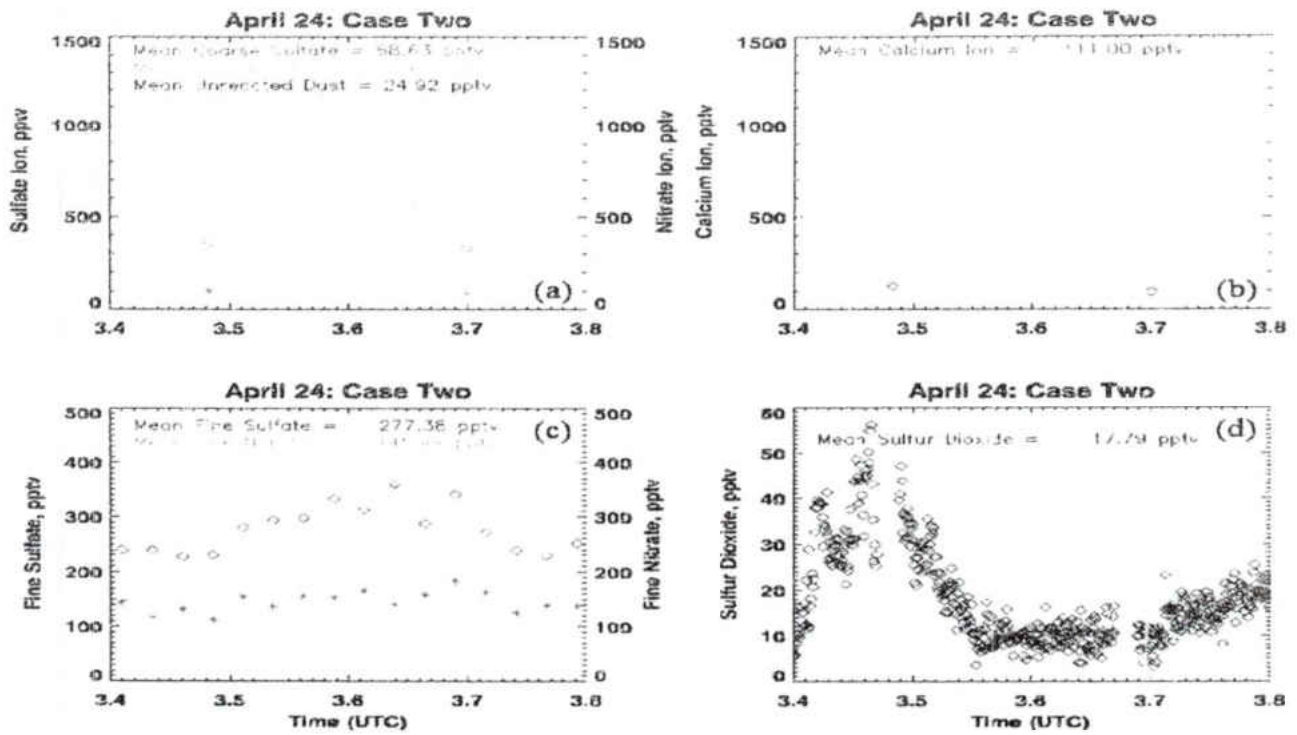


Figure 22: April 24 Case

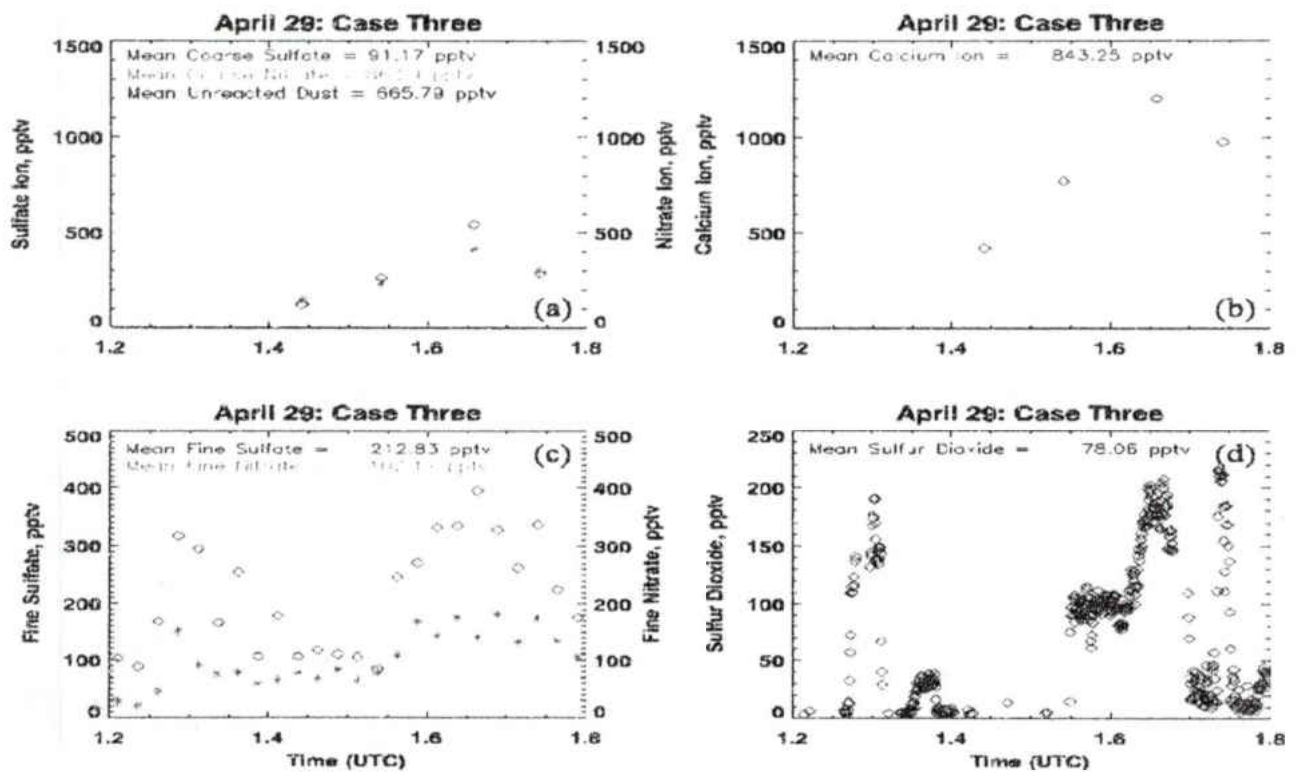


Figure 23: April 29 First Plume Case

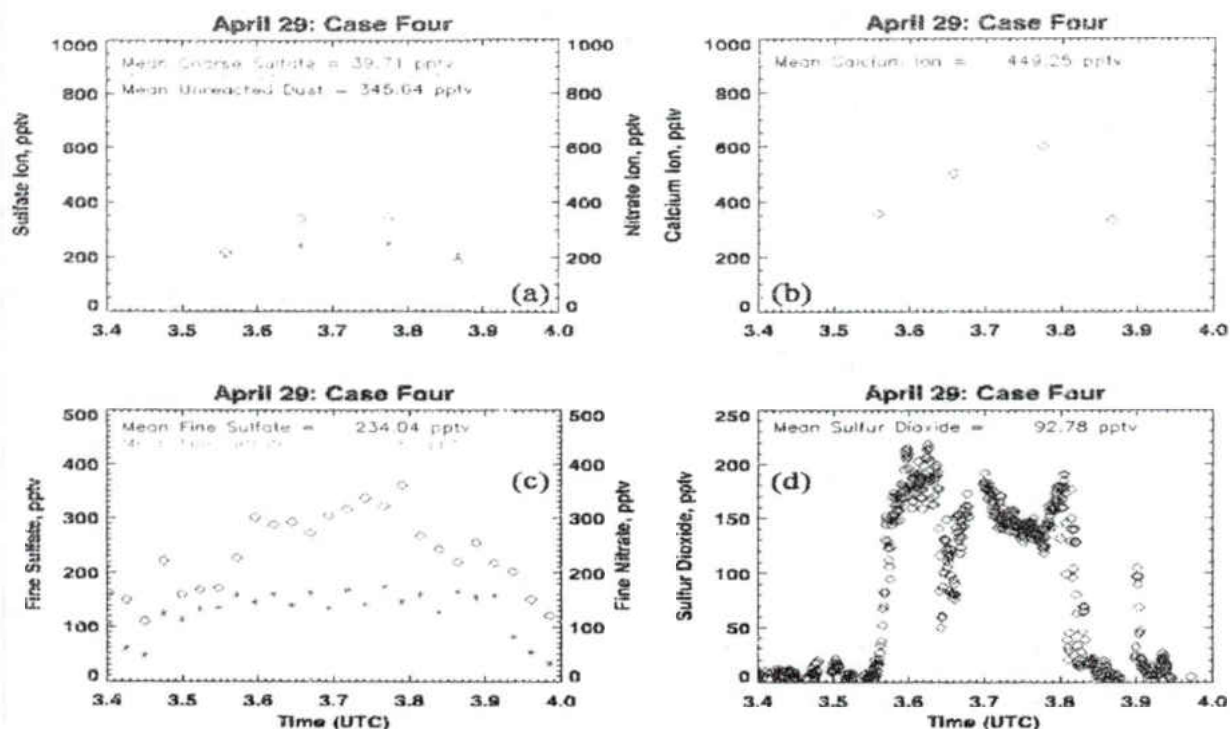


Figure 24: April 29 Second Plume Case

Results and Discussion

Figures 21 to 24 show the other pollution components (e.g. fine mode nitrate, SO_2) and the derived soluble coarse mode sulfate and nitrate in the plume. Both Case I and II had very low SO_2 mixing ratios in the plume (both with less than 20 ppbv), which suggested that either formation process of sulfate aerosol had taken place well before the measurements or perhaps there was no such process during the transport. Also for Cases I and II, there were no correlations between the SO_2 and sulfate aerosol. These analyses were consistent with the conclusion in Chapter III. That is, when the plume for Case I exited the Asian continent, it did not pass through many large urban regions which lead to low mixing ratios of both SO_2 and particulate aerosols. When the plume for Case II exited the Asian continent, it passed through numerous urban areas which lead to elevated mixing ratios of particulate pollution. The left over SO_2 mixing ratios were low

in the plume, which supported our assumption of the gas phase to particulate phase conversion taking place before the plume reached the remote eastern Pacific because the dust plume cannot just carry the particulate phase pollutions without mixing the gas phase pollutions. The SO₂ mixing ratios of Cases III and IV were much higher than Cases I and II, and SO₂ and sulfate aerosol were well correlated (not shown in the diagram). This further indicated that much higher gas phase pollution existed in the plume.

	Mean [Coarse SO ₄ ²⁻] (pptv)	Mean [Coarse NO ₃ ⁻] (pptv)	Mean [Ca ⁺⁺] (pptv)	Mean [Unreacted Dust] (pptv)
Case I	115.43	78.80	272.00	117.17
Case II	68.63	34.89	111.00	24.92
Case III	91.17	172.58	843.25	665.79
Case IV	39.71	127.80	449.25	345.64

Table 3: Mean Unreacted Dust Fractions for Cases I-IV

Table 3 summarizes the results for Cases I – IV. The generation of secondary pollutants at the cost of Asian dust and gaseous precursors is related to the unreacted calcium fraction left behind after the reaction. Cases I and II had relatively low unreacted fractions at 117.17 and 24.92 pptv, respectively, which suggests a more complete gas to particulate phase reaction mechanism that took place in plume which left behind very little unreacted Asian dust as compared to the calcium concentrations. Cases III and IV had very large amount of unreacted fractions with values of 665.79 and 345.64 pptv, respectively. The elevated levels of sulfur dioxide mixing ratios suggest an incomplete gas to particulate phase reaction during plume transport. This presents an inherent contradiction since more dust should generate more secondary pollution in the coarse

mode as pointed out by previous studies referenced in this study. However, those studies did not take into account the amount of unconverted gas phase pollution that may be present within the dust plume.

The Third Scientific Question

Comparison of the dust and pollution vertical distribution among 3 field experiments in the remote Pacific region

With both the increased frequency of Asian dust events during the spring season and human activities during the past two decades, the two field campaigns prior to INTEX-B (PEM-B and TRACE-P) were compared and summarized by Dibb et al., (2003). Their study examined if there were significant differences of measured calcium, sulfate, ammonia and nitrate mixing ratio between PEM-B and TRACE-P. However, in order to investigate the third question, we adopted the analysis method used by Dibb et al., 1996, 1997 and 2003. They utilized a binning and averaging method in order to show the collocation of Asian pollution with Asian dust. They used four height bins to simulate four hypothetical parts of the atmosphere: (1) less than 1 km denotes the boundary layer, (2) between 1 and 6 km denotes the lower troposphere, (3) between 6 and 9 km denotes the middle troposphere, and (4) all levels greater than 9 km denote the upper troposphere. The pollution tracers (sulfate, nitrate and ammonium) as well as dust tracer data (calcium) are averaged over the height intervals such that a vertical distribution is obtained.

Figure 25 shows the vertical distribution of dust and pollution of all measurements at remote Pacific region during INTEX-B (called 'mean_remote_Pacific' on the diagram), PEM-B (1994) and TRACE-P (2001) campaigns. The vertical distribution of calcium did show the highest mixing ratio among the three experiments, and the mixing ratio for all three components during INTEX-B are much higher than the other 2 experiments except at lowest height bin (i.e. the boundary layer). The mixing ratios of the three pollution tracers during INTEX-B were much lower than those during

TRACE-P and higher than those during PEM-B. One of the strongest reasons is the measurements during INTEX-B happened at much far away from the Asian continent compared to the other two experiments, therefore, the plume during INTEX-B experienced a much longer transport time as compared to the other two experiments. As a result, less pollution tracers should be found in the boundary layer as compared with the free atmosphere.

However, within the boundary layer, sea salt aerosols can react with the Asian pollution and dust to form coarse mode pollution as well. Sea salt particles can behave in much the same way as Asian dust particles in generating reaction sites for heterogeneous reactions to occur, and these reactions deplete the gas phase pollutants in the lowest height bin. It is important to note that the standard deviations for all four mixing ratios during INTEX-B (Figure 25) are large, and the further investigation may need to improve the quality of the data. If the measurements are equally reliable for all three experiments then Figure 25 suggests three things: (a) increased pollution loading during plume transport processes due to pollution data, (b) the intensity of the dust plume has increased since the last two campaigns due to dust data, and (c) better sampling methods and techniques could yield better results.

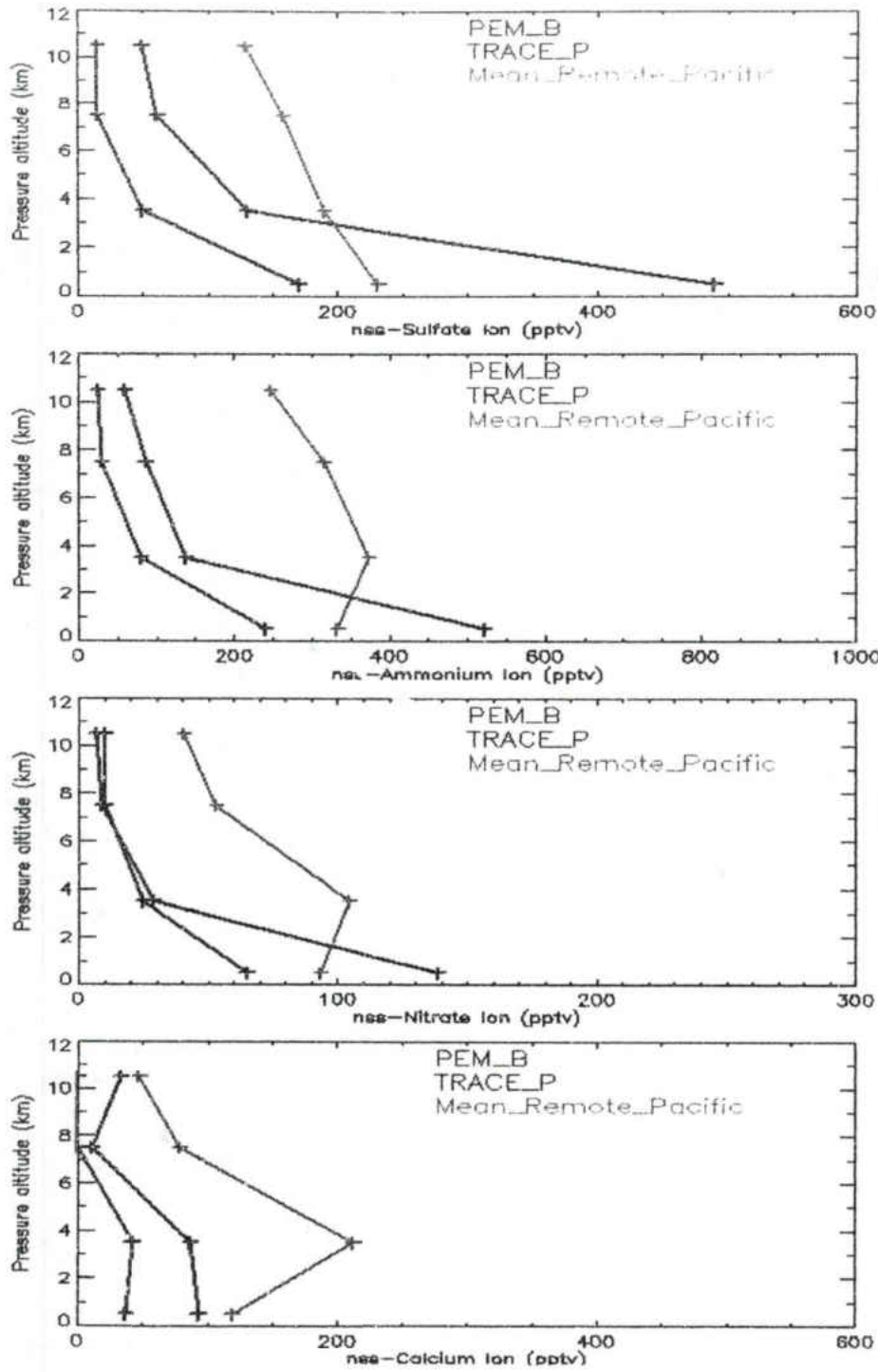


Figure 25: Vertical distribution of mean Asian dust and pollution values over the remote eastern Pacific.

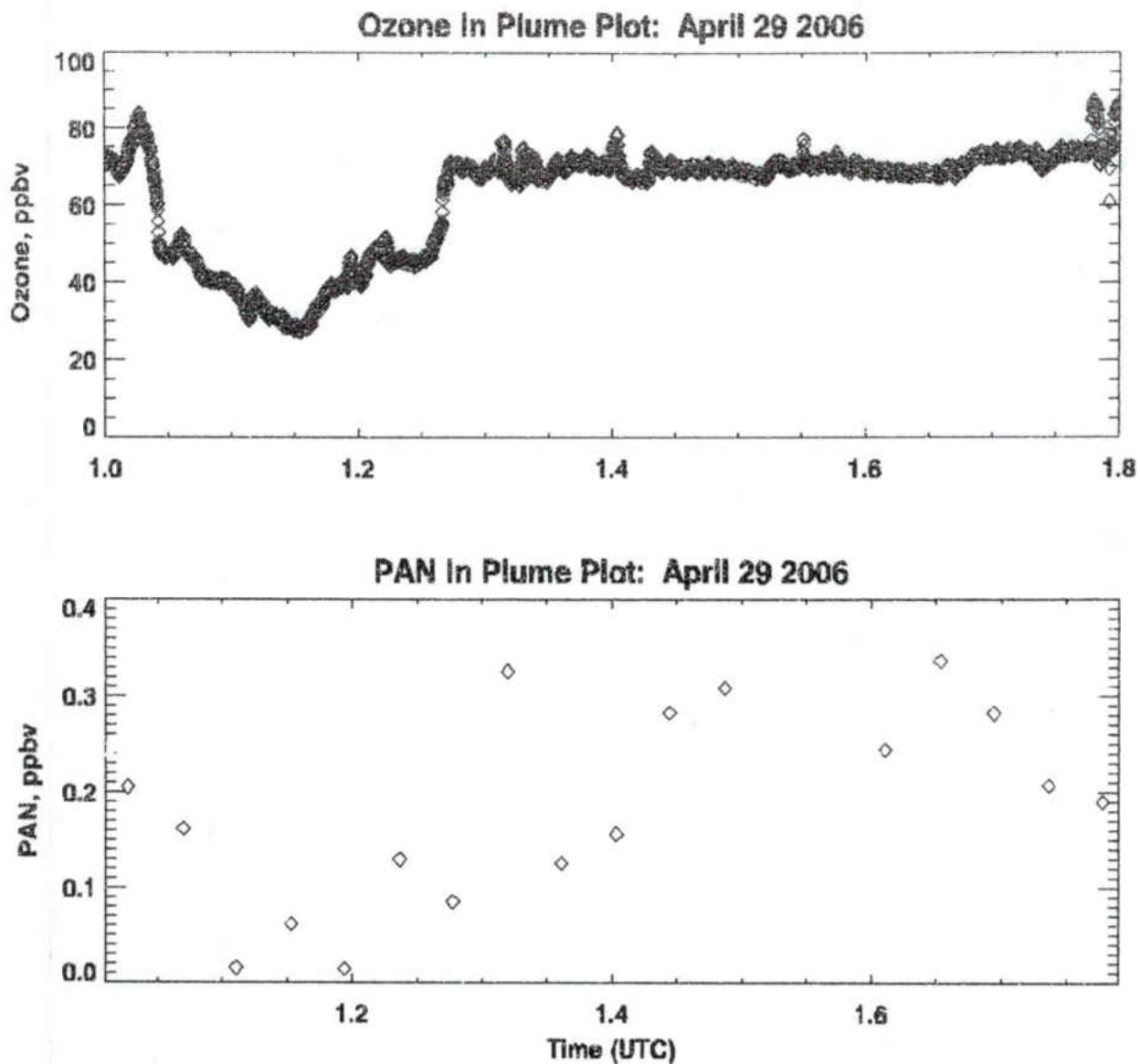


Figure 26: Temporal Relationship between PAN and Ozone in April 29 Case

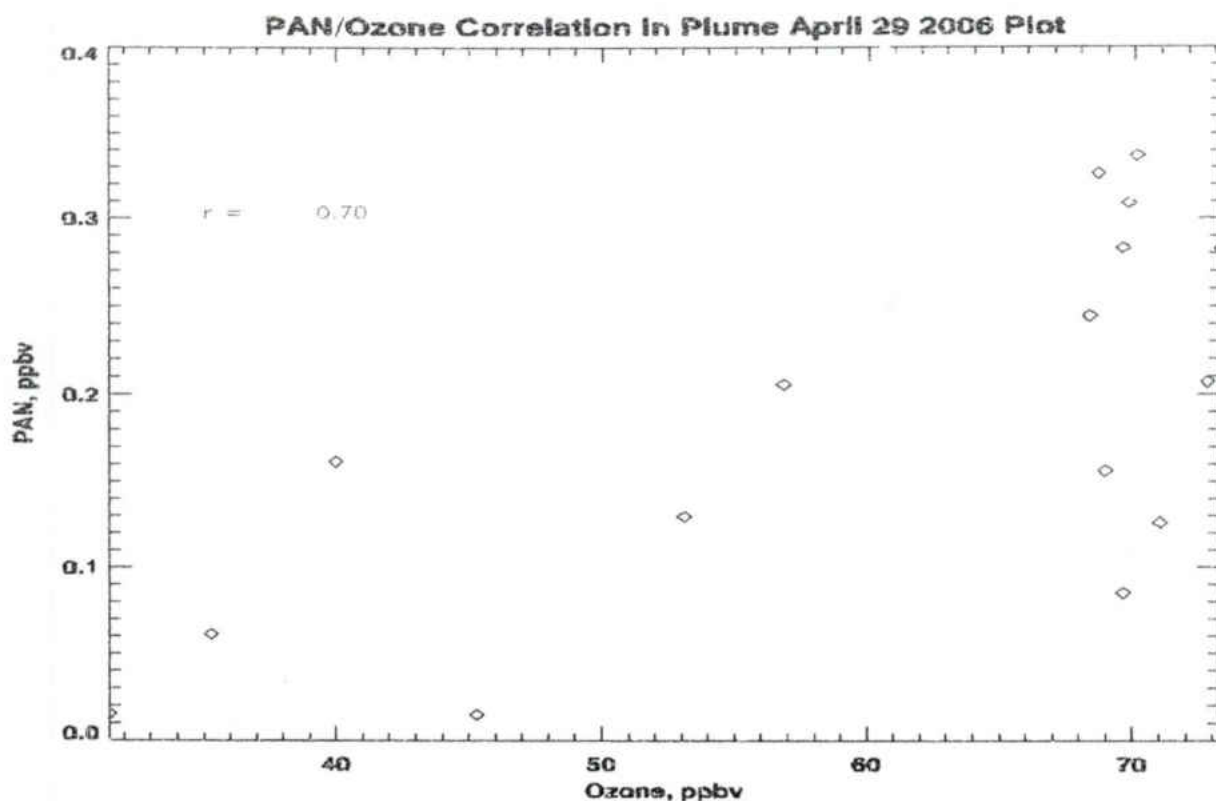


Figure 27: Statistical Correlation of PAN with Ozone during the April 29 Case

Relationship between PAN and Ozone within the dust plume

There are other reactions that are occurring in the plume as indicated by Eq. 1.5 (a-c). Figures 26 and 27 show the temporal and statistical relationships between PAN and ozone in Case II. The temporal plot shows both PAN and ozone trends that match between hour 1.05 and 1.25 UTC. Ozone levels decrease with a corresponding decrease in PAN levels. Data analysis revealed a strong correlation between the two compounds within the plume ($r = 0.7$) during this time interval. Note that Case II also had the highest values of calcium in all four cases which suggests an enhancement of ozone formation by PAN. This contrasts with the clean case where there was a weaker correlation ($r = 0.3$) while the mean calcium concentrations were well below background values.

CHAPTER IV

CONCLUSIONS

Dust events observed over the remote eastern Pacific were found to contain varying amounts of Asian pollution. After the initiation of the dust events on the Asian continent, they then passed over heavily polluted regions, lofted pollution into the atmosphere, then traveled eastward across the Pacific Ocean. In this study, the use of in situ measurements and back-trajectory model output data has established a direct relationship between the dust and pollution plume. Four case studies were used to illustrate this connection by using atmospheric scattering ratios, as shown by the “in plume” results in Chapter III: (a) Case I is dominated by dust particles with calcium mixing ratio greater than 200 pptv, Angström exponent less than 1, fine aerosol sulfate mixing ratio less than 100 pptv, (b) Case II is dominated by pollution plume with calcium mixing ratio 111 pptv, fine aerosol mixing ratios close to 280 pptv, Angström exponent much greater than 1, and (c) Cases III and IV had the dust and pollution co-existing as given by calcium concentrations of 843 and 449 pptv, respectively, fine aerosol concentrations near 220 pptv, and Angström exponent less than 1. In all four cases the spectral curvature was negative suggesting any intrusion of fine aerosol will influence the spectral nature of the dust plumes.

A clean, dust free case was used along with the same four case studies used in addressing Question Two. The clean case had either weak or negligible concentrations of dust in a flight track that is at the same altitude as a nearby dust plume as given by the

DIAL plot (Fig 12b). One main finding of this analysis is although the presence of dust does facilitate coarse mode pollution generation, strong dust events do not necessarily mean strong generation of coarse mode nitrate and sulfate aerosols (i.e. coarse mode pollution). Case III and Case IV both had strong dust loading as given by calcium ion mixing ratios much greater than 200 pptv. The unreacted dust fraction resulted in being 79% and 77%, respectively, the total reacted dust fraction (as given by the mean calcium mixing ratio). In both these cases sulfur dioxide mixing ratios exceeded 200 pptv (though the mean ratios were close to 100 pptv) which suggests a large fraction of unconverted gas phase pollution. In Cases I and II, the unreacted dust fractions were 43% and 21%, respectively, while the sulfur dioxide mixing ratios were well below 100 pptv which suggests more of a complete reaction between Asian dust and aqueous mode pollution.

In addition to the results outlined in the previous paragraph, Cases I and II had very low SO₂ mixing ratios within the plume, while Cases III and IV had elevated SO₂ mixing ratios. Since the emission over the Asian continent cannot have significant daily variation, the differences among the plume cases containing such different pollution mixing ratios can be explained by: (a) the plume has different pathway over the continent, and (b) the process of chemical reactions involving depletions of gas phase pollution within the plume is different. Three out of four cases, with the exception of Case I, had the similar pollutant pathways over the center of China, as given by their back trajectory analysis. Therefore, reason (a) may be ruled out for the difference of chemical compositions in the plumes. The reactions for Case II have been completed in terms of SO₂ conversion to sulfate aerosols, but there are still sufficient amounts of SO₂ in

Cases III and IV for further reactions to take place within the dust plume along its transport pathway. If any dust plumes similar to Cases III and IV reach the North America, then significant pollutions such as sulfate aerosols and SO₂ may be observed.

A comparison between the PEM West B (1994) and TRACE-P (2001) campaigns is shown in Fig. 25. These campaigns sampled Asian outflow in the western remote Pacific and just off the Asian mainland. There is a slight increase in the amount of secondary pollution along with Asian dust (as given by their chemical tracers, sulfate, nitrate and ammonium for secondary Asian pollution; calcium for Asian dust) between these campaigns as shown by the vertical distribution plots. This would verify a collocation of Asian dust with Asian pollution. These campaigns are compared with the INTEX-B (2006) study. Note that since no new pollution is being added to the dust plumes as they exit the Asian mainland and travel eastward, the findings in the second part of this study suggested that the increases in pollution are occurring much farther east in the remote Pacific during INTEX-B (2006) as compared to the other two studies. For example, nitrate ion mixing ratios show a near fivefold increase in the remote Pacific lower troposphere over previous levels given in the two earlier campaigns.

However, Dibb et al. (2003) in their comparison study between PEM-B (1994) and TRACE-P (2001), suggested that the observed enhancements may be due to the DC-8 aircraft measuring well organized Asian outflow using better sampling techniques and methods (Dibb et al., 2003). This may also be the case with the comparison between INTEX-B (2006) and the two previous studies and their corresponding data. As a result, extensive error analysis may be needed to verify that there is actually an increase in dust

and pollution outflow from Asia as well as more source observations of the dust plumes before they leave the Asian continent.

The temporal plots of PAN and ozone show a close inter-relationship within the dust plume. Though the generation of ozone from PAN (and vice versa) cannot be found one to one relationship in this study, Fig. 26 does show a similar trend in mixing ratios of both gas phase pollutants. The correlation (Fig. 27) between the two also shows at least a collocation and further analysis would need to be done to state for certain if one is responsible for the generation of the other.

From this study, the HYSPLIT back-trajectory data indicated two possible source regions of the Asian dust: the Gobi desert and Tibetan plateau; both are vast regions of terrain that are continuing to undergo desertification processes. The model results were also consistent to the NCEP global reanalysis (not shown in this thesis). The HYSPLIT data also showed how the paths of the dust events passed over large populated and industrialized areas of Asia. This finding is slightly different from former study which utilized solely physical properties of Asian dust events along with a forward trajectory model.

The data used in this study has not had extensive error analysis because only a few cases met our selection criteria. More field experiments may be needed to address any similar questions as the questions we raised in this study. Also, further investigation may be needed for determining the microphysical properties of fine and coarse modes within the dust plume. Though the use of scattering ratios and in situ measurements lead to the aforementioned conclusions, the effects of fine mode pollution, especially the

secondary pollution need to be completely understood to determine its role in terms of climate, air quality and human health effects.

REFERENCES

- Adams, F. and X.D. Liu (2009), Characterization of three atmospheric aerosol episodes at a coastal site in China: Implications for regional transport of air pollution, *Eur. Phys. J. Conferences 1*, 211-223 (2009).
- Albrecht, B.A., (1989), Aerosols, Cloud microphysics, and Fraction Cloudiness. *Nature*, 245, 1227-1230.
- Anderson, Theodore L. and Ogren, John A.(1998), Determining Aerosol Radiative Properties Using the TSI 3563 Integrating Nephelometer, *Aerosol Science and Technology*, 29:1,57-69.
- Arimoto, R., Y.J. Kim, P.K. Quinn, T.S. Bates, T.L. Anderson, S. Gong, I. Uno, M. Chin, B.J. Huebert, A.D. Clarke, Y. Shinozuka, R.J. Weber, J.R. Anderson, S.A. Guazzotti, R.C. Sullivan, D.A. Sodeman, K.A. Prather, I.N. Sokolik (2006), Characterization of Asian Dust during ACE-Asia (2006), *Global and Planetary Change 52* (2006) 23-56.
- Castillejos, M., Borja-Aburto, V.H. Dockery, D.W., Gold, D.R., Loomis, D., 2000. Airborne coarse particles and mortality. *Inhalat. Toxicol.* 12 (Suppl. 1), 61-72.
- Dibb, J.E., R.W. Talbot, K.I. Klemm, G.L. Gregory, H.B. Singh, J.D. Bradshaw, and S.T. Sandholm, Asian influence over the western North Pacific during the fall season: Inferences from lead 210, soluble ionic species, and ozone, *J. Geophys. Res.*, 101, 1779-1792, 1996.

- Dibb, J.E., R.W. Talbot, B.L. Lefer, E. Scheuer, G.L. Gregory, E.V. Browell, J.D. Bradshaw, S.T. Sandholm, and H.B. Singh (1997), Distributions of beryllium 7 and lead 210, and soluble aerosol-associated ionic species over the western Pacific: PEM West B, February – March 1994, *J. Geophys. Res.*, Vol 102, No. D23, Pages 28,287-28302, December 20, 1997. Dibb, J.E., R.W. Talbot, E.M. Scheuer, G. Seid, M.A. Avery and H.B. Singh, (2003), Aerosol chemical composition in Asian continental outflow during the TRACE-P campaign Comparison with PEM-West B, *J. Geophys. Res.*, Vol 108, No. D21, 8815.
- Dockery, D.W., Schwartz, J., Spengler, J.D., 1992. Air pollution and daily mortality: associations with particulates and acid aerosols. *Environ. Res.* 59, 362-373.
- Fang, X., Han Yongxiang, MA Jinghui, Song Lianchun, Yang Shengli, and Zhang Xiaoye, 2004. Dust Storms and loess accumulation on the Tibetan Plateau: A case study of dust event on 4 March 2003 in Lhasa, *Chinese Science Bulletin* 2004, Vol. 49, No. 9, 953-960.
- Frisch, A.S., C.W. Fairall, and J.B. Snider, 1994, Measurement of Stratus Cloud and Drizzle Parameters in ASTEX with a Ka-Band Doppler Radar and Microwave Radiometer, *J. Atmos. Sci.*, Vol. 52, 2788-2799.
- Gobbi, G.P., Kaufman, Y.J., Koren, I., and Eck, T.F., (2007), Classification of aerosol properties derived from AERONET direct sun data, *Atmos. Chem. Phys.*, 7, 453-458.

- Guzzi, R., Elsa Cattani, Marco Cervino, Chiara Levoni, Francesca Torricella (2005, January 21). *Aerosol Optical Thickness from GOME data. Methodological approach and preliminary results. 3rd ERS Symposium Florence 97*. Retrieved May 31, 2009 from <http://earth.esa.int/workshops/ers97/papers/guzzi/>
- Husar, R. B., D. M. Tratt, B. A. Schichtel, S. R. Falke, F. Li, D. Jaffe, S. Gassó, T. Gill, N. S. Laulainen, F. Lu, M. C. Reheis, Y. Chun, D. Westphal, B. N. Holben, C. Gueymard, I. McKendry, N. Kuring, G. C. Feldman, C. McClain, R. J. Frouin, J. Merrill, D. DuBois, F. Vignola, T. Murayama, S. Nickovic, W. E. Wilson, k. Sassen, N. Sugimoto, and W. C. Malm (2001), Asian dust events of April 1998, *J. Geophys. Res.*, 106(D16), 18 317-18 330.
- Jacob D.J., Jennifer A. Logan and Prashant P. Murti (1999), Effect of rising Asian emissions on surface ozone in the United States, *Geophysical Research Letters*, Vol. 26, No. 14, Pages 2175-2178, July 15, 1999.
- Jaffe D., Theodore Anderson, Dave Covert, Robert Kotchenruther, Barbara Trost, Jen Danielson, William Simpson, Terje Bernsten, Sigrun Karlsdottir, Donald Blake, Joyce Harris, Greg Carmichael, and Itsushi Uno (1999), Transport of Asian Air Pollution to North America, *Geophysical Research Letters*, Vol. 26, No. 6, Pages 711-714, March 15, 1999.
- Jaffe D., Julie Snow, and Owen Cooper (in press). The 2001 Asian Dust Events: Transport and Impact on Surface Aerosol Concentrations in the U.S., *EOS*, Vol. 84, No. 46, 18 November 2003, Pages 501-516.
- Jordan, C.E., J.E. Dibb, B.E. Anderson, and H.E. Fuelberg, Uptake of nitrate and sulfate on dust aerosols during TRACE-P, *J. Geophys. Res.*, 108(D21), 8817.

- Leaitch, W.R., A.M. Macdonald, K.G. Anlauf, P.S.K. Liu, D. Toom-Sauntry, S.M. Li, J. Liggio, K. Hayden, M.A. Wasey, L.M. Russell, S. Takahama, S. Liu, A. van Donkelaar, T. Duck, R.V. Martin, Q. Zhang, Y. Sun, I. McKendry, N.C. Shantz, and M. Cubison, 2009, Evidence for Asian dust effects from aerosol plume measurements during INTEX-B 2006 near Whistler, BC, *Atmos. Chem. Phys.*, *9*, 3523-3546, 2009.
- Levy, J.I., Hammitt, J.K., Spengler, J., 2000. Estimating the mortality impacts of particulate matter: what can be learned from between-study variability? *Environ. Health Perspect.* *108*, 109-117.
- Liu, 1985 T.S. Liu, Loess and the Environment. *China Ocean Press*, Beijing (1985) p. 251.
- McNaughton, C. S., Clarke, A. D., Kapustin, V., Shinozuka, Y., Howell, S. G., Anderson, B. E., Winstead, E., Dibb, J., Scheuer, E., Cohen, R. C., Wooldridge, P., Perring, A., Huey, L. G.,²⁰ Kim, S., Jimenez, J. L., Dunlea, E. J., DeCarlo, P. F., Wennberg, P. O., Crouse, J. D., Weinheimer, A. J., and Flocke, F.: Observations of heterogeneous reactions between Asian pollution and mineral dust over the Eastern North Pacific during INTEX-B, *Atmos. Chem. Phys. Discuss.*, *9*, 8469–8539, 2009, <http://www.atmos-chem-phys-discuss.net/9/8469/2009/>.
- Qu, W.J., Xiao Y. Zhang, Richard Arimoto, Dan Wang, Ya Q. Wang, Li W. Yan, and Yang Li (2008), Chemical composition of the background aerosol at two sites in southwestern and northwestern China: potential influences of regional transport, *Tellus* (2008), *60B*, 657-673.

- Sassen (1991), The Polarization Lidar technique for cloud research: A review and current assessment, *BAMS*, 72, 1848-1866.
- Schwartz, J., Dockery, D.W., Neas, L.M., 1996. Is daily mortality associated specifically with fine particles? *J. Air Waste Manage. Assoc.* 46, 927-939.
- Singh, H. B., W. H. Brune, J. H. Crawford, H. Fuelberg, and D. J. Jacob (2005), *The Intercontinental Chemical Transport Experiment – Phase B (INTEX-B): An update*, Retrieved October 5, 2006, from NASA LaRC website: [http://cloud1.arc.nasa.gov/docs/intex-na/INTEX-B_White_Paper.pdf].
- Stith, J. L., et al. (2009), An overview of aircraft observations from the Pacific Dust Experiment campaign, *J. Geophys. Res.*, 114, D05207.
- Ware, J.H., Thibodeau, L.A., Speizer, F.E., Colome, S. and Ferris, B.G., 1981. Assessment of the health effects of atmospheric sulphur oxides and particulate matter: evidence from observational studies. *Environ. Health Perspect.* 41, pp. 255–276.
- Xin, J., et al. (2007), Aerosol Optical Depth (AOD) and Angström exponent of aerosols observed by the Chinese Sun Hazemeter Network from August 2004 to September 2005, *J. Geophys. Res.*, 112, D05203.
- Yong-Shing Chen, Pai-Ching Sheen, Eng-Rin Chen, Yi-Kuen Liu, Trong-Neng Wu, and Chun-Yuh Yang (2003), Effects of Asian dust storm events on daily mortality in Taipei, Taiwan, *Environmental Research* 95 (2004) 151-155.
- Young Yoo, Ji Tae Choung, Jinho Yu, Do Kyun Kim, Young Yull Koh (2008), Acute Effects of Asian Dust Events on Respiratory Symptoms and Peak Expiratory Flow in Children with Mild Asthma, *J. Korean Med Sci* 2008; 23: 66-71.

- Zhang, M., I. Uto, G. R. Carmichael, H. Akimoto, Z. Wang, Y. Tang, J-H Woo, D. G. Streets, G. W. Sachse, M. A. Avery, R. J. Weber, and R. W. Talbot, (2003), Large-scale structure of trace gas and aerosol distributions over the western Pacific Ocean during TRACE-P, *J. Geophys. Res.*, Vol **108**, No. D21, 8820.
- Zhuang H., Chak K. Chan, Ming Fang, Anthony S. Wexler, (1999), Formation of nitrate and non-sea-salt sulfate on coarse particles, *Atmospheric Environment* 33 (1999) 4223-4233.